Charles University in Prague

Faculty of Science

Department of Cell Biology

Bc. Karolina Ditrychova

The role of *DISP3* gene in cell proliferation

Role genu *DISP3* v buněčné proliferaci

Master´s thesis

Supervisor: Mgr. Martina Zikova, CSc.

Prague, 2016

I declare, that this thesis is my original work and that it has not been previously submitted to obtain any other degree. All sources of information are cited properly in the Reference section.

Part of the results was obtained from or in cooperation with Mgr. Jana Konirova, Laboratory of Cell Differentiation, Institute of Molecular Genetics AS CR.

Prague, 29.4.2016

Karolina Ditrychova

Acknowledgement

I would like to acknowledge my supervisor, Martina Zikova, CSc., for her guidance, support and a lot of patience during whole my studies and mainly during the preparation of this thesis. Next, I would like to thank to Jana Konirova, who helped me a lot with overexpression experiments. Besides, many thanks belong also to all members of our laboratory for useful suggestions and advice, mainly to Jana Oltova for helpful advice with CRISPR-Cas9 system. Special acknowledgment belongs also to Petr Bartunek, CSc. for opportunity to participate on projects in his laboratory and for good piece of advice. Finally, I would like to acknowledge my family, friends and mainly my partner for their support and patience during whole my studies.

List of Abbreviations

3-HMG-CoA	3-hydroxy-3-methylglutaryl-Coenzyme A
7-DHCR	7-dehydrocholesterol reductase
BDNF	Brain-derived neurotrophic factor
BSA	Bovine Serum Albumin
cpm	counts per minute
CRISPR	Clustered Regularly Interspaced Short Palindromic Repeats
CTNNB1	β-catenin
DISP1	Dispatched 1
DISP3	Dispatched 3
DMEM	Dulbecco´s Modified Eagle Medium
EGL	external germinal layer
EPB4.1L3	Loss of erythrocyte membrane protein band 4.1 –like 3
ER	endoplasmic reticulum
ERK ½	Extracellular regulated kinase 1/2
FBS	Fetal Bovine Serum
FISH	fluorescence *in situ* hybridization
FW	forward
GABA	γ-Amminobutyric acid
GAPDH	Glyceraldehyde-3-phosphate dehydrogenase
GFAP	Glial fibrillary acidic protein
HH	Hedgehog
HS	Horse Serum
LDL	Low density lipoprotein
MAPK	Mitogen-activated protein kinase

MEM	Minimum Essential Medium
NGF	Nerve growth factor
NGS	Normal Goat Serum
NHEJ	Non-homologous end joining
NPC1	Niemann-Pick type C protein 1
NPC1L1	Niemann-Pick type C protein 1 – like 1
PCR	Polymerase chain reaction
P/S	Penicilin/Streptomycin
PEI	Polyethylenimine
PI3K	Phosphatidylinositol-3-kinase
PRELP	Proline/arginine-rich end leucine-rich repeat protein
PTC	Patched
qRT-PCR	quantitative reverse transcription polymerase chain reaction
rpm	revolutions per minute
RT-PCR	reverse transcription polymerase chain reaction
RV	reverse
SCAP	SREBP cleavage activating protein
SHH	Sonic Hedgehog
SLOS	Smith-Leimli-Opitz syndrom
SREBP	Sterol response element binding protein
SSD	Sterol-sensing domain
T3	Thyroid hormone
TRUP1	Thyroid hormone-upregulated protein 1
WNT	Wingless

For purpose of this thesis, we use human gene nomenclature. Genes are indicated by italicized letters, proteins are indicated by regular letters.

Abstract

Dispatched 3 (DISP3), sterol - sensing domain (SSD) – containing protein, is a key focus of our laboratory. It was described as a gene regulated by thyroid hormone and its expression is mainly localized within neural tissue. Our preliminary data suggested increased DISP3 expression in medulloblastoma, a highly common pediatric cerebellar tumour, therefore we wanted to examine DISP3 role in human cancer cells.

The aim of this thesis is to perform DISP3 overexpression and downregulation in human medulloblastoma cell lines and in mouse neural progenitors and analyse its effect on cell proliferation and differentiation. For this purpose, we chose DAOY and D341, human medulloblastoma cell lines with low and high expression of DISP3 and mouse multipotent neural progenitor cell line, C 17.2, with low DISP3 expression.

We showed, that DISP3 ectopic expression leads to increase in cell proliferation in both DAOY and C 17.2 cells. Next, we examined the ability of C 17.2 cells to differentiate into neurons and astrocytes and observed, that cells overexpressing DISP3 reveal delay in differentiation, what we proved by analysis of cell specific markers.

Using CRISPR-Cas9 targeting system, we reduced DISP3 expression within D341 cells and observed decrease in their proliferation. Finally, we analysed cell cycle profile of DISP3-downregulated D341 cells.

Key words: Dispatched 3 (DISP3), cancer, proliferation, differentiation

Abstrakt

Jedním z hlavních projektů naší laboratoře je výzkum funkce proteinu Dispatched 3 (DISP3). Tento protein se řadí do rodiny proteinů obsahujících sterol sensing doménu (SSD). Gen, který ho kóduje, byl dříve popsán jako regulovaný thyroidním hormonem a k jeho expresi dochází především v neurální tkáni. Naše nepublikovaná data ukazují jeho zvýšenou hladinu v meduloblastomech, velice častých nádorech mozečku u nezletilých. Na základě těchto zjištění jsme začali studovat roli DISP3 v lidských rakovinných buňkách.

Cílem této práce je sledovat vliv zvýšené nebo snížené exprese DISP3 na buněčnou proliferaci a diferenciaci jednak v lidských buněčných liniích, jednak v myších neurálních progenitorech. Za tímto účelem jsme si vybrali buněčné linie DAOY a D341 pocházející z lidských meduloblastomů, které se výrazně liší mírou exprese DISP3, a linii myších neurálních multipotentních progenitorů C 17.2, v nichž je DISP3 exprimován velmi slabě.

Ukázali jsme, že zvýšená exprese DISP3 v buněčných liniích DAOY a C 17.2 vede ke zvýšení buněčné proliferace. Dále jsme diferencovali buněčnou linii C 17.2 do neuronů a astrocytů a sledovali, že buňky se zvýšenou expresí DISP3 projevují menší ochotu podstoupit diferenciační proces, což jsme následně potvrdili pomocí specifických markerů.

Za použití CRISPR-Cas9 systému jsme snížili expresi DISP3 v buněčné linii D341 a následně ukázali, že tento pokles vede ke snížení buněčné proliferace. Na závěr jsme zanalyzovali profil buněčného cyklu v populacích buněk D341 se sníženou expresí DISP3.

Klíčová slova: Dispatched 3 (DISP3), rakovina, buněčná proliferace, buněčná diferenciace

1. Introduction

Dispatched 3 (DISP3) was identified in our laboratory during the screen for thyroid hormone-regulated genes. DISP3 protein consists of 13 transmembrane domains and belongs to the family of sterol sensing-domain (SSD)-containing proteins (Zikova, Corlett et al. 2009).

SSD-containing proteins have distinct roles within cell and organism - they play role in cholesterol uptake and transport as well as in cholesterol metabolism regulation. Some members of the family are also key players in cell signalling (Kuwabara and Labouesse 2002). DISP3 protein is localized in endoplasmic reticulum and it is supposed to link thyroid hormone regulation with cholesterol metabolism (Zikova, Corlett et al. 2009).

DISP3 is predominantly expressed in the brain and the retina, less in the testis. In my thesis, I will focus on its expression in cerebellum, where DISP3 is localized mainly within Purkinje cells (Zikova, Corlett et al. 2009). As our preliminary data show, DISP3 expression is elevated in medulloblastoma tumour samples, which suggest its role in medulloblastoma formation or maintenance.

Medulloblastoma is a highly common pediatric tumour, which arise within cerebellum. Medulloblastoma is subdivided into four molecular subgroups, which differ in their cell and molecular origin and reveal different prognosis (Samkari, White et al. 2015). It was observed that dysregulation of distinct neurodevelopmental processes may lead to formation of medulloblastoma (Schuller, Heine et al. 2008, Gibson, Tong et al. 2010) and thus it reveals the question whether DISP3 may be also involved in this dysregulation.

In this thesis I ask whether DISP3 dysregulated expression in medulloblastoma cell lines has effect on cell proliferation, as it is one of the major properties of cancer cells. In addition, I also analyse the effect of DISP3 ectopic expression on neural progenitor cells and their ability to undergo differentiation process.

2. Literature overview

2.1 Dispatched 3 gene/protein

Dispatched 3 (*DISP3*, also known as *PTCHD2*, *KIAA1337* and *TRUP 1- Thyroid hormone up-regulated 1*; deposited in Genbank with accession number EU429800) was first described by *in silico* study (Katoh and Katoh 2005). By later screening for novel thyroid hormone (T3) -regulated genes performed in our laboratory, *DISP3* was found as gene regulated by T3 treatment in avian erythroid progenitor cells (Zikova, Corlett et al. 2009). Chicken transcript is 4017 bp long and gives rise to the protein consisting of 1338 amino acids with molecular weight about 150 kDa. Alignment of the chicken sequence reveals 87% of homology and 80 % of identity with mouse form, and 84 % of homology and 78% of identity with human form. Topology prediction used to characterize protein structure revealed, that DISP3 contains 13 transmembrane domains, five of which form so-called sterol sensing-domain (SSD). This domain is situated in N-terminal part of the protein among second to sixth transmembrane domains (Figure 2.1). Phylogenetic analysis revealed relationship of DISP3 to members of SSD-containing family (Kuwabara and Labouesse 2002), in which can be found important players in cholesterol metabolism regulation and cholesterol linked signaling (Figure 2.2).

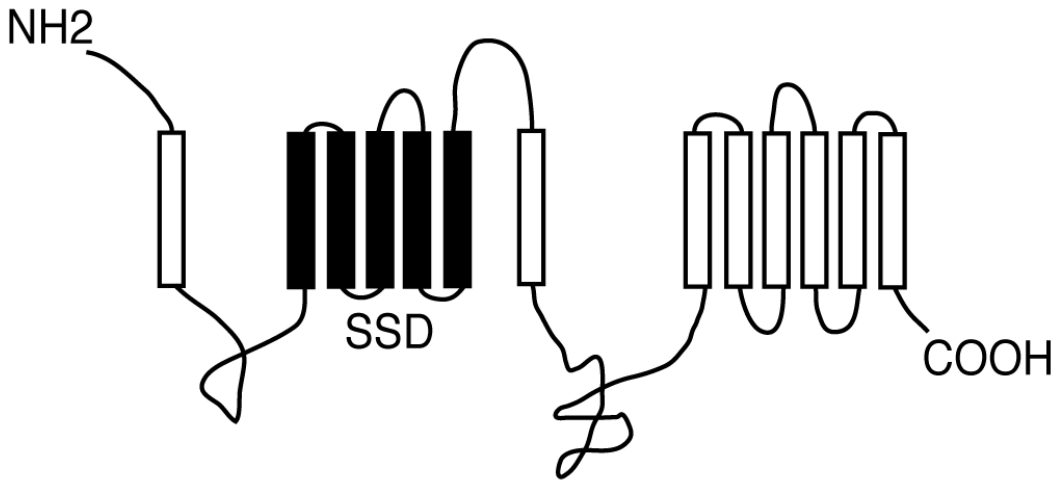

Figure 2.1. Scheme of DISP3 structure. Transmembrane domains are visualized as boxes, SSD is in the black colour. The protein is localized in the membrane of endoplasmic reticulum (Zikova, Corlett et al. 2009).

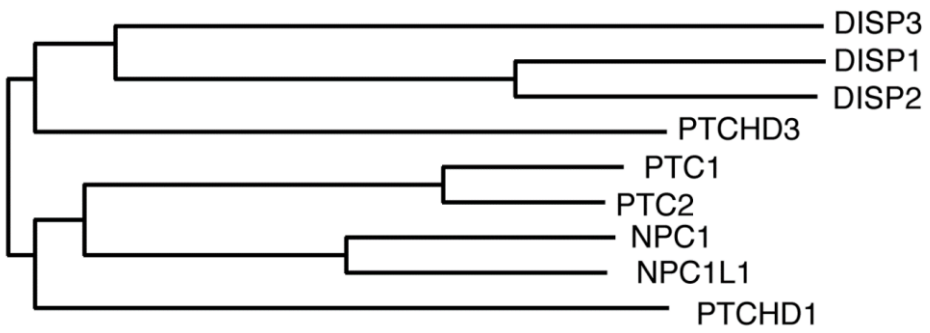

Figure 2.2. Phylogeny tree of DISP3. It reveals close relationship of DISP3 to members of SSD-containing family (Zikova, Corlett et al. 2009).

DISP3 expression was studied in mouse and chicken adult tissues. DISP3 expression in chicken was mainly observed in brain, retina, testis and thymus, with less abundancy in the spleen and the kidney. In mice, its expression was predominantly situated in the neural tissue and only weak expression in the bone marrow and the testis was observed. To analyze which cell subtypes reveal DISP3 expression *in vivo*, immunohistochemical staining of the retina and the brain tissue was performed. Its expression was found in inner nuclear layer of the retina, specifically in ganglion and bipolar cells of retina. In the brain, DISP3 reveals expression mainly in hippocampus (region CA1-CA3) and cerebellum (Purkinje cells), also with scattered localization within the cortex. (Zikova, Corlett et al. 2009).

2.2 Thyroid hormone regulation of DISP3

Thyroid hormone, secreted by thyroid glands, is an important molecule playing role in correct development of many tissues in both pre- and postnatal development, and affecting cell proliferation and differentiation. Dysregulation of thyroid hormone signalling may lead to many dysfunctions as dwarfism, thyroid cancer or various metabolism abnormalities as reviewed in (Cho 2015, Gutleb, Cambier et al. 2016). *In vivo* analysis performed in our laboratory showed thyroid hormone dependent DISP3 down-regulation in chicken ganglion cells in the retina, without any perturbation of embryonal development. Further studies with different cell lines were performed *in vitro.* DISP3 expression was found in human retinoblastoma, mouse hippocampal progenitor and in Sertoli-like cell lines. Its regulation by

thyroid hormone was shown to be different in each cell line, depending on cell origin. While thyroid hormone treatment of retinoblastoma increases DISP3 expression more than five times, in Sertoli-like cells it causes decrease in DISP3 expression almost three times. It shows, that DISP3 expression in different cell types responds to T3 treatment in different way (Zikova, Corlett et al. 2009).

Thyroid hormone absence during fetal neurodevelopment results in decrease of cortical thickness. Diminished proliferation and increased apoptosis within neuron progenitor cells together with cell cycle arrest and changes in transcription were observed. These results suggests, that thyroid hormone is a key regulator of neural progenitor proliferation and differentiation (Mohan, Sinha et al. 2012). Similar effects were observed within cerebellum, where T3 transport was disrupted. Decrease of cerebellar cortical thickness was observed as well as defects in synapsis formation and axon myelination (Lopez-Espindola, Morales-Bastos et al. 2014).

The thyroid hormone can affect cell signalling through cytoplasm, cytosol, nuclear or mitochondrial receptors and may function by genomic or non-genomic pathway. In non-genomic pathway, it transduces signal through cytoplasm integrin receptors to Mitogen-activated protein kinase (MAPK) and Extracellular regulated kinase 1/2 (ERK1/2) pathway, or Phosphatidylinositol-3-kinase (PI3K) pathway regulating cell proliferation and differentiation. Genomic pathway of thyroid signalling transduce signal directly to nuclear thyroid receptors, which serve in unliganded form as transcriptional repressors or activators (Cheng, Leonard et al. 2010, Hammes and Davis 2015). T3 effect was found to be crucial not only in developing nervous system, but also in other tissues, such as pancreas or testis as reviewed in (Lucas, Nascimento et al. 2014, Mastracci and Evans-Molina 2014, Preau, Fini et al. 2015). Mechanism of thyroid hormone regulation of Disp3 was studied in our laboratory. We analysed thyroid hormone receptor binding sites within *DISP3* genomic locus, however, we did not obtain any conclusive results (data not published).

2.3 Potential role of DISP3 in cholesterol metabolism

2.3.1 DISP3 has effect on cholesterol level *in vitro*

When expression of DISP3 was analyzed in tissue and cell subtypes, DISP3 localization in cell was found to be restricted to the endoplasmic reticulum and outer nuclear membrane in both endogenous and ectopic expression. Because DISP3 protein reveals similarity with proteins acting in cholesterol metabolism and transport, and moreover, it contains specific SSD, which was found to interact with cholesterol (Nohturfft, Brown et al. 1998), cholesterol amount in cells was measured. Compared to control cells, approximately 30% increase in cholesterol level in cells ectopically expressing DISP3 was found (Figure 2.3). While in control cells cholesterol is mainly located in plasma membrane, in the cells with DISP3 ectopic expression cholesterol is localized in the endoplasmic reticulum (ER) and its distribution overlaps with DISP3 protein ectopic expression. Furthermore, when cells were transfected with DISP3 lacking its SSD, only slight increase in cholesterol amount was observed (Zikova, Corlett et al. 2009).

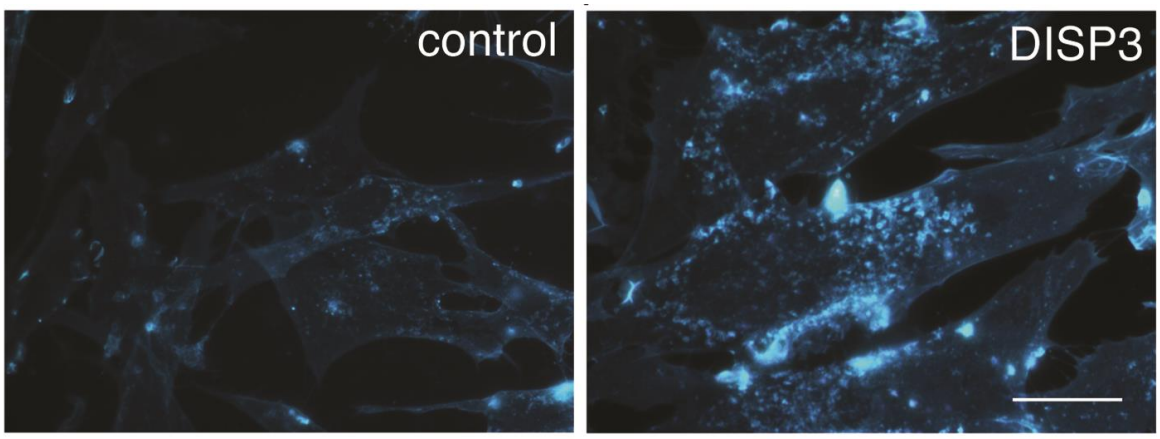

Figure 2.3. DISP3 overexpression leads to increase of cholesterol amount in the cell compared to control – filipin staining of cholesterol (Zikova, Corlett et al. 2009).

These findings together with its domain phylogeny links DISP3 with SSD-containing protein family. Although one subcategory of these proteins is involved in cholesterol-linked Hedgehog (HH) signaling, the rest of the proteins act in cholesterol synthesis, regulation of cholesterol metabolism or in its transport within cell (Kuwabara and Labouesse 2002).

2.3.2 SSD-containing proteins and cholesterol metabolism

2.3.2.1 SSD-containing protein family

The SSD-containing family is a group of transmembrane proteins with different function within the cell. They are linked in different ways with the cholesterol molecule and its distinct roles in cell metabolism and signaling. The SSD-containing protein family can be subdivided into three distinct subgroups, based on their role in the cell. The first group contains proteins playing role in cholesterol trafficking and uptake. This group consists of Niemann-Pick type C protein 1 (NPC1) and Niemann-Pick type C protein 1 – like 1 (NPC1L1).

The second group of SSD-containing proteins is involved in cell signaling. Proteins Patched (PTC) and Dispatched 1 (DISP1) are key regulators of Hedgehog pathway and are localized on plasma membrane. HH molecule is a protein with two posttranslational modifications – palmitic acid and cholesterol are bound to the HH molecule. PTC is responsible for signal income and DISP1 acts in releasing of HH molecule from the cell.

The last group of SSD-containing proteins plays role in regulation of cholesterol metabolism in the cell. It contains 3-hydroxy-3-methylglutaryl-Coenzyme A (3-HMG-CoA) reductase, the key enzyme in cholesterol synthesizing mevalonate pathway and its regulatory protein - Sterol response element binding protein (SREBP) cleavage-activating protein (SCAP) (Kuwabara and Labouesse 2002).

2.3.2.2 Cholesterol molecule

Cholesterol is the key molecule in cell metabolism and structure. It is important constituent of the plasma membrane, where it affects membrane properties such as fluidity and rigidity or fusion of membrane vesicles. While it may interact with hydrophobic residues of membrane components due to its hydrophobic aromatic ring, hydroxyl group at the other part of the cholesterol molecule can interact with hydrophilic environment. Although cholesterol synthesis takes part mainly in the endoplasmic reticulum, its major location in the cell is in the plasma membrane. Thus many ways of cholesterol transport in the cell are involved. Cholesterol can be translocated by direct binding to the specific proteins between different cellular membranes, or can be transferred by vesicular trafficking in the cell as reviewed in (Brown and Goldstein 2009, Wustner and Solanko 2015).

Cholesterol content in the cell may be maintained by its uptake due to its receptors on the plasma membrane – Low density lipoprotein (LDL) receptors (Brown, Faust et al. 1975) or synthesized by so-called mevalonate pathway (Goldstein and Brown 1990). Both of these processes are strictly regulated by cholesterol itself and major regulators comes from SSD-containing protein family (Brown and Goldstein 2009).

2.3.2.3 Cholesterol synthesis

The key enzyme in cholesterol synthesis is 3-HMG-CoA reductase, which converts 3-HMG-CoA to mevalonate. This transmembrane protein is localized in the endoplasmic reticulum (Liscum, Cummings et al. 1983, Liscum, Luskey et al. 1983, Liscum, Finer-Moore et al. 1985). Its expression and protein turnover is particularly regulated by SREBP/SCAP protein complex, because cleavage activation of transmembrane transcription factor SREBP is required for its translocation into the nucleus.

When cholesterol is present in the cell, SCAP binds with cholesterol molecule and together they form complex with SREBP. The complex is localized within the endoplasmic reticulum, where SREBP cannot be cleaved. However, if cholesterol amount is low, the cholesterol molecule does not bind to SREBP/SCAP complex and both proteins are transported to the Golgi apparatus, where SREBP is cleaved and thus activated (Wang, Sato et al. 1994, Sakai, Duncan et al. 1996, Duncan, Brown et al. 1997, Sakai, Nohturfft et al. 1997, Nohturfft, Brown et al. 1998, Nohturfft, DeBose-Boyd et al. 1999). The cleaved SREBP then translocate to the nucleus, where it functions as a transcription factor of many genes involved in cholesterol metabolism (Hua, Yokoyama et al. 1993, Yokoyama, Wang et al. 1993).

Another enzyme, which contains SSD and plays important role in cholesterol synthesis, is called 7-dehydrocholesterol reductase (7-DHCR) and it converts cholesterol precursor, 7-dehydrocholesterol, to cholesterol (Moebius, Fitzky et al. 1998, Bae, Lee et al. 1999).

2.3.2.4 Cholesterol uptake

The process of cholesterol uptake can be both LDL particle dependent and LDL particle non-dependent. Within the LDL particle-dependent uptake, LDL particles are endocytosed and cholesterol transfer inside the endosomal/lysosomal vesicle is dependent on Niemann-Pick type C 1 protein (Kwon, Abi-Mosleh et al. 2009). Furthermore, another SSD-containing was found to be involved in cholesterol LDL non-dependent uptake into the cell within the intestine and was characterized as Niemann-Pick type C 1-like 1 protein (Altmann, Davis et al. 2004).

2.3.3 Cholesterol linked disorders and SSD-containing proteins

Since cholesterol is the key molecule with many important roles in both cell and organism, such as constituent of membranes or precursor of several hormones, its proper regulation is required. When the regulatory mechanism described above is failing, metabolic or developmental disorders affecting mainly neural tissues can occur. Two disorders linked with SSD-containing proteins were described, Niemann-Pick disease type C and Smith-Leimli-Opitz syndrome (SLOS).

Niemann-Pick disease type C was described as neural disorder (Vanier 2015). This disease is caused by mutation mainly in gene *NPC1*. Molecular effect of this mutation was shown as accumulation of cholesterol in late endosomes and lysosomes, because NPC1 is responsible for cholesterol efflux in these organelles. In *NPC1* null mice, beside neuronal malformation increase of cholesterol level was found in neuronal cells, especially in Purkinje cells in cerebellum (Lopez, Klein et al. 2011). Similar to Niemann-Pick disease, SLOS is caused by mutation in SSD-containing protein and affects cholesterol content in the cell. In SLOS, there is mutation in *7-DHCR*, which leads to accumulation of cholesterol precursor, however, cholesterol itself is lacking in the organism. In contrast to Niemann-Pick disease, in SLOS variety of different tissue is affected (Patrono, Rizzo et al. 2000).

Based on our previous findings that DISP3 affects amount and localization of cholesterol in the cell, together with fact that it is expressed mainly in neural tissue, where cholesterol content in plasma membrane is even higher than in other tissue, we started to ask whether

DISP3 could also play role in neural tissue properties. In my project I focus on DISP3 function in neural tissue-derived cell cultures with the aim to understand its role in cell proliferation and differentiation.

2.4 DISP3 role in neural tissue proliferation and differentiation

2.4.1 DISP3 expression in neural tissue

DISP3 is mainly expressed in the neural tissue and its expression in context of the brain was observed in Purkinje cells in cerebellum and in hippocampus within CA1-CA3 region and dentate gyrus and also weak expression pattern in cortex (Zikova, Corlett et al. 2009). Moreover, high expression level of DISP3 was observed in several brain tumor samples, with increased expression mainly in medulloblastoma samples (data not published). These data suggested an idea, that DISP3 may regulate cell proliferation within the cell. In this thesis, I use human medulloblastoma cell lines – DAOY and D341, to perform overexpression and knock-out studies and observe Disp3 role in proliferation regulation. Since not only proliferation, but also differentiation plays important role in tumor development and progression, we decided to use neural progenitor cell line C17.2, to perform differentiation experiments.

2.4.2 Medulloblastoma

Medulloblastoma tumor is a common type of high-grade brain cancer derived from the cerebellum. The age of patients suffering this disorder is unfortunately low and prognosis remains poor, although therapy approach improved and survival ratio have increased to 70%. However, common occurrence of metastasis, reaching 30% of patients, reveals poor prognosis of this high-risk group. Main treatment approach for medulloblastoma remains surgery followed by radiotherapy combined with chemotherapy, which often brings often side effects such as dementia, risk of early stroke or metastatic dissemination. Therapeutic subdivision of medulloblastoma based on histopathology was established into four groups: classic, large cell/anaplastic, desmoplastic/nodular cell and extensive nodularity

medulloblastoma (Khatua 2016). DISP3 overexpression was observed across all of these subtypes (oncomine.org).

Furthermore, medulloblastoma was divided into specific subtypes based on the molecular classification. Four different classes were established, that diverse in cell origin, tumor driving mutations and in its prognosis: Wingless (WNT), Sonic Hedgehog (SHH), subgroup 3 and subgroup 4. First, WNT group of medulloblastoma, with its almost 100% survival rate and non-metastatic manner, reveals activating mutation in WNT canonical pathway leading to non-physiological accumulation of β-catenin in the cell nucleus and thus driving tumor progression. Immunohistochemistry staining of β-catenin thus could be good prognostic marker of this cancer subtype and also inhibition of WNT signaling pathway possible clinical approach (Samkari, White et al. 2015). In WNT medulloblastoma group mice model, mutation driving tumor progression was described in *CTNNB1* gene and its cellular origin was determined in dorsal brainstem (Gibson, Tong et al. 2010).

In contrast, SHH medulloblastoma subclass reveals distinct cellular origin as it was shown, that Sonic Hedgehog canonical pathway activating mutations lead to medulloblastoma formation in mice (Yang, Ellis et al. 2008) and (Schuller, Heine et al. 2008). Prognosis for SHH subtype of medulloblastoma depends on additional risk factors such as p53 mutation or SHH-independent amplification of GLI and its accumulation in the nucleus. These additional markers significantly lower the survival rate to 20-30% of patients within 5 years. However, transgenic mice model for this cancer subtype promise new therapeutic approach as the new specific inhibitors are tested.

Whereas WNT and SHH subgroups are well described, subgroup 3 and 4 are less defined with several overlaps. Group 3 has unfortunately very poor prognosis, patients mostly suffer metastatic progression and thus are classified as high-risk. Hallmark of subgroup 3 medulloblastoma is amplification of MYC together with specific genetic aberrations.

Subgroup 4 of medulloblastoma is the least described subgroup with any further classification, main marker of this subgroup is Potassium voltage-gated channel subfamily A member 1 protein. Although patients of all ages were diagnosed with medulloblastoma, unfortunately subfamily 4 mainly affects children. For further classification of this cancer subtype, combination of several immunohistochemistry and FISH molecular markers is

needed. Some tumors reveal MYC amplification with then poor prognosis, while other subcategory shows loss of chromosome 11 and gain of chromosome 17, revealing low-risk properties. Based on poorly defined manner of subgroup 3 and 4 formation, there is no promising targeted therapy in contrast with WNT or SHH subgroups, however high-throughput therapeutic screens are bringing new possibilities (Samkari, White et al. 2015).

In our laboratory, we focused on DISP3 expression in different brain tumor samples. Analysis revealed high expression in medulloblastoma cancer in consistency with previous findings (oncomine.org). Comparison of different medulloblastoma patient samples among their molecular subtypes revealed expression of DISP3 mainly in subcategory 4, with less expression in SHH subcategory (preliminary data, Figure 2.4).

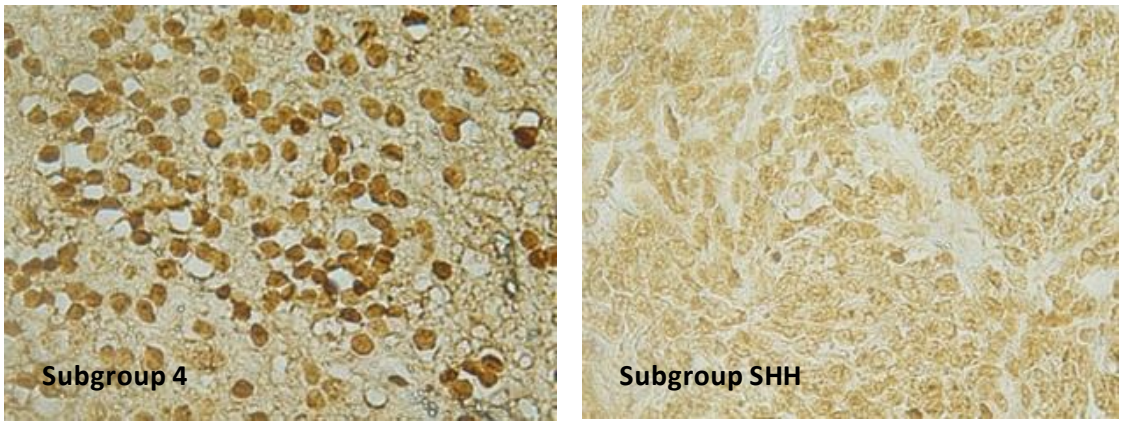

Figure 2.4. DISP3 immunohistological staining in distinct molecular subgroups of medulloblastoma. Subgroup 4 (on the left) reveals higher expression of DISP3 (dark colour in the left picture).

2.4.3 DAOY and D341 cell lines

In my experiments, we were looking for medulloblastoma cell lines with both high and low expression of DISP3 to perform up- and down-regulation studies. In our depository, we had DAOY cell line expressing low level of DISP3 (preliminary data). This cell line comes from human medulloblastoma sample with categorization to desmoplastic group of medulloblastoma tumors. It was derived from 4 years old male brain tumor in 1985, however, it reveals loss of Y chromosome in its tetraploid karyotype. It was shown to be able to form tumors when xenotransplanted into mice. Although the original cell culture

revealed ability to undergo both neuronal and glial differentiation, DAOY cell line cannot be differentiated to glial-like cells anymore (Jacobsen, Jenkyn et al. 1985) and (atcc.org).

In contrast to DAOY cell line, D341 cells express significantly high level of DISP3 (preliminary data), which makes them suitable for down-regulation experiments. D341 cell line was also derived from human medulloblastoma samples, from 3,5 years old male patient in 1988, and is also able to form tumors after xenotransplantation to mice. These cells grow in suspension and are capable of forming spheres. The cell line expresses neuroectodermal markers and high amount oncogenic c-MYC, in consistency with common MYC expression in human medulloblastoma subtypes (Friedman, Burger et al. 1988). Both these cell lines have original doubling time more than 30 hours, specifically DAOY 34 hours and D341 37 hours (atcc.org).

2.4.4 Differentiation role in medulloblastoma formation

It was observed that medulloblastoma arise within neural progenitor subpopulation (Schuller, Heine et al. 2008). Hence, it is not so surprising to find neural stem properties among different tumor samples. During analysis of several pediatric brain tumors was found that medulloblastoma maintain stem-like properties when cultured *in vitro*, where it forms neurospheres. These derived cells are still repeatedly able to form tumors after xenotransplantations to mice. Moreover, with different success, they are also capable of differentiation to neuronal and glial cell subtypes, suggesting idea, that tumor progression in this cancer involves block of differentiation and the maintaining stem-like properties (Hemmati, Nakano et al. 2003, Singh, Clarke et al. 2003). Therefore, we decided to test abilities of DISP3 to affect differentiation of cerebellar neural progenitor cells.

2.4.5 Neurogenesis in cerebellum

Cerebellum is part of the brain, which is responsible for sensor and motoric activity. Moreover, it also plays cognitive role affecting several key functions such as speech, attention or emotional behaviour. The cerebellum consists of limited number of cell types,

which are localized in specified layers. In the developed cerebellum, there is established architecture of tissue consisting of molecular and granule layers, Purkinje cells monolayer and cerebellar nuclei neurons zone. Most subpialy, there is localized molecular layer consisting of dendritic trees of Purkinje cells together with axon fibres of granule cells. It is separated from granule layer, where bodies of granule cells are localized, by monolayer of Purkinje cells. At the bottom, there are localized cerebellum nuclei neurons (Marzban, Hoy et al. 2015).

Neurogenesis in the cerebellum is localized in two distinct zones called ventricular zone and rhombic lip, which give rise to distinct cellular subtypes. While ventricular zone produces GABAergic neuronal populations, rhombic lip gives rise to glutamatergic neurons. Ventricular zone of the cerebellum, in consistency with cortical ventricular zone of neurogenesis, produces neural progenitors, which migrate radially through cerebellum body and give rise to Purkinje cells and stellate, basket, Golgi and Lugaro interneurons (Butts, Chaplin et al. 2011). During cortical neurogenesis, there are neural stem cells in ventricular zone, producing radial glia by asymmetrical division. Radial glia were also shown to be capable of differentiation to both neuronal or glia cell subtypes. Radial glia migrate to subventricular zone, where they undergo further asymmetrical or symmetrical division to increase the number of intermediate neural progenitors. Those cells then give rise to mature neurons or glia (Laguesse, Peyre et al. 2015). Cerebellar ventricular zone neurogenesis was suggested to bear similar features as cortical neurogenesis, however exact mechanism has yet to be elucidated.

The second zone of cerebellar neurogenesis was defined as rhombic lip, which produces neuronal subtypes such as granule cells or unipolar brush cells. Within rhombic lip, there are temporaly distinct ways of neurogenesis giving rise to different cell populations. First, progenitors of deep nuclei cells are produced, then they migrate tangentially and subpialy and then they radially transverse to deep cerebellar nuclei zone. Second, neurogenesis of rhombic lip gives rise to granule cells precursors, which also migrate tangentially above pial surface. Afterwards, granule cell precursors undergo massive proliferation to form so-called external germinal layer (EGL). Proliferation in EGL is caused by SHH signal, which is produced by already established Purkinje cells layer. It was suggested that dysregulation of this mechanism leads to medulloblastoma formation. At last, rhombic lip neurogenesis produce

unipolar brush cell precursors, which also migrate to external germinal layer, where the both precursors undergo differentiation and migration to their specified localization in the granule layer. Although all these mechanism starts early in embryogenesis, definitive formation of cerebellar architecture is finished postnataly, human cerebellum architecture is established during first two years (Butts, Chaplin et al. 2011).

2.4.6 C 17.2 cells and their differentiation

In my experiments, I use mouse neural progenitor cells C 17.2 to observe their differentiation upon DISP3 overexpression. C 17.2 cells were derived from cerebellar external germinal layer, which makes them good model for experiments studying DISP3 effect on differentiation properties. C 17.2 cells were derived by retroviral transduction of *v-myc* in dissociated mice cerebellum cells. After selection, several clones were tested for their properties. C 17.2 clone was described as cell line capable of differentiation to neuron-like and glia-like cell subtypes with ability to be transplanted to developing cerebellum (Snyder, Deitcher et al. 1992). In *in vitro* conditions, C 17.2 cells are capable of differentiation to neurons and astrocytes when treated with N2 supplement, brain-derived neurotrophic factor (BDNF) and nerve growth factor (NGF) (Lundqvist, El Andaloussi-Lilja et al. 2013).

To prove differentiation to distinct neural cell subtypes, specific biomarkers are used, on both mRNA and protein levels. Neural progenitors are commonly characterized by production of Nestin, type IV intermediate filament (Frederiksen and McKay 1988, Dahlstrand, Lardelli et al. 1995). Neurons are defined by expression of a cytoskeletal protein, β-III tubulin, that is localized in axons and dendrites of neuron, although it is produced in neuron body (Roskams, Cai et al. 1998). Finally, to detect astrocytes, Glial fibrillary acidic protein (GFAP), cytoskeletal protein from the type III intermediate filament family, is used (Eng, Vanderhaeghen et al. 1971, Bignami and Dahl 1974).

3. Materials and Methods

3.1 Materials

3.1.1 Vectors and constructs

pBabe - Hygro - Disp3

pBABE-Hygro (Plasmid No. 1765 – AddGene) is retroviral expressing vector with hygromycin resistance. The full length human *DISP3* cDNA was cloned to the pBABE-Hygro vector and the construct was called pBabe-Hygro-DISP3. It was obtained from M. Zikova, Ph.D. and used for over-expression experiments.

pCDNA3 - DISP3

pCDNA3 is mammalian expressing vector with neomycin resistance. The full-length human *DISP3* cDNA was cloned to the pCDNA3 vector and the construct was called pCDNA3-DISP3. It was obtained from M. Zikova, Ph.D. and used for over-expression experiments.

pGEM-T Easy Vector System I

pGEM-T is linearized vector with thymidine overhangs used to subclone of PCR products (Promega).

pLentiCRISPR-Loop1.1, -Loop1.2, -Loop1.3, Loop1.4, -SSD4, -SSD5

pLentiCRISPRv1 (Plasmid No. 49535 - AddGene) is vector with puromycin resistance, expressing Cas9 enzyme and CRISPR gRNA (Shalem, Sanjana et al. 2014). Different oligonucleotides (Loop1.1, Loop1.2, Loop1.3, Loop1.4, SSD4 and SSD5) were cloned into the pLentiCRISPRv1 as templates for CRISPR gRNA expression and these constructs were called pLentiCRISPR-Loop1.1, pLentiCRISPR-Loop1.2, pLentiCRISPR-Loop1.3, pLentiCRISPR-Loop1.4, pLentiCRISPR-SSD4 and pLentiCRISPR-SSD5. These constructs were used for knock-out experiments.

pCMV-VSV-G

Vector pCMV-VSV-G (Plasmid No. 8454 – AddGene) encodes envelope proteins for lentiviral particle. Used in co-transfection with psPAX2 and pLentiCRISPR construcst to prepare lentiviral particles.

psPAX2

Vector psPAX2 (Plasmid No. 12260 – AddGene) encodes packaging proteins of lentiviral particle. Used in co-transfection with pCMV-VSV-G and pLentiCRISPR constructs to prepare lentiviral particles.

3.1.2 Enzymes

Restriction enzymes, DNA ladder and T4 ligase used for work with recombinant DNA were obtained from Promega, New England Biolabs and Fermentas.

3.1.3 Bacteria and growing media

Bacteria: *Escherichia coli* strain TOP 10 (Invitrogen), fast growing strain used for amplification of plasmids.

LB medium: 1% tryptone, 1% yeast extract, 1% NaCl

LB agar: 1.5% agar in LB

Selective antibiotics:

Ampicilin (Sigma-Aldrich) in final concentration 100 μg/ml.

3.1.4 Eucaryotic cell lines

HEK Phoenix-ECO

Human embryonic kidney adherent cell line used for retroviral particles packing. Cell line already contains Adeno- and SV40 viral sequences (ATCC® CRL-3214™).

HEK 293 FT

Human embryonic kidney adherent cell line with stable expression of SV40 large T antigen. It is used for lentiviral particles production.

C 17.2

Mouse adherent neural progenitor cell line, derived from cerebellar tissue (Snyder, Deitcher et al. 1992).

DAOY

Human medulloblastoma cell line (ATCC® HTB-186™).

D341

Human medulloblastoma cell line (ATCC® HTB-187™).

3.1.5 Media and reagents for eukaryotic cells

Reagents:

Dulbecco's Modified Eagle Medium (DMEM), Gibco ref. 11885-084

Improved Minimum Essential Medium (Improved MEM), Gibco ref. 10373-017

DMEM Nutrient Mixture F-12 HAM (DMEM:F12), Sigma-Aldrich ref. D8062

Fetal Bovine Serum (FBS), Gibco ref. 10270-160

Horse Serum (HS), Gibco ref. 26050088

Normal Goat Serum (NGS), Gibco ref. PCN5000

L-Glutamin, Gibco ref. 25030-024

Penicilin/Streptomycin mixture (P/S), Gibco ref. 15140-122

N2 Supplement, Gibco ref. 17502-048

Brain-derived neurotrophic factor (BDNF), R&D Systems ref. 248-BD-005

Nerve growth factor (NGF), R&D Systems ref. 1156-NG-100

Opti-MEM, reduced serum medium, Gibco ref. 11058021

Lipofectamine®2000 Reagent, Invitrogen ref. 11668019

Geneticin (G418), Thermo Fisher Scientific, ref. 10131027, 200-350 µg/ml

Puromycin, Thermo Fisher Scientific, ref. A1113803, 300 ng/ml

Media:

HEK Phoenix-Eco and HEK 293 FT

DMEM, 10% of FBS, 2% L-Glutamin, 1% P/S

C 17.2

DMEM, 10% FBS, 5% HS, 1% L-Glutamin, 1% P/S, 7 ml Glucose (25%)

C 17.2 differentiating medium

DMEM:F12, 1% N2 supplement, 10 ng/ml BDNF, 10 ng/ml NGF

DAOY, D341

Improved MEM, 10% FBS, 1% P/S

3.1.6 CRISPR gRNA oligonucleotides

Target sequences were selected by http://www.e-crisp.org/E-CRISP/ webpage, complementary sequences were then designed and BsmBI overhangs were added. Oligonucleotides with BsmBI overhangs were ordered, annealed and cloned into pLentiCRISPR vector. All designed oligonucleotides were obtained from Sigma-Aldrich.

Loop1.1:

5‘- CACCGAAGCGTCTCGGAGGTGAAGT – 3‘ and 5‘- AAACACTTCACCTCCGAGACGCTTC – 3‘

Loop1.2:

5‘-CACCGCTGCCAGATCCTCCAGGGGC – 3‘ and 5‘-AAACGCCCCTGGAGGATCTGGCAGC – 3‘

Loop1.3:

5‘-CACCGTTGCTCAGCCGCTGGTTTCG – 3‘ and 5‘-AAACCGAAACCAGCGGCTGAGCAAC – 3‘

Loop1.4:

5‘-CACCGGGTAGACTGCTTGGCCAGCA – 3‘ and 5‘-AAACTGCTGGCCAAGCAGTCTACCC – 3‘

SSD4:

5‘-CACCGAGCTGCTGCTGATGAAGGCC – 3‘ and 5‘-AAACGGCCTTCATCAGCAGCAGCTC – 3‘

SSD5:

5‘-CACCGCGAAGGCGGCCACCCCATTC – 3‘ and 5‘-AAACGAATGGGGTGGCCGCCTTCGC – 3‘

3.1.7 Primers

All primers were designed by http://www.ncbi.nlm.nih.gov/tools/primer-blast/ webpage and obtained from Sigma-Aldrich.

The following primers were used for T7 endonuclease assay and sequencing:

Loop1.1:

FW: 5´-TACTACCCACCGCTGGACAT-3´ and RV: 5´-TTTCGCGGGTCTTCACTCTG-3´

Loop1.2, Loop1.3:

FW:5´- CTTCACCTCCGAGACGCTT-3´ and RV:5´- AGTAGGTCATGAGCGAGCTG-3´

Loop1.4:

FW:5´- GGCTGCAATGAGACTGGATG-3´ and RV: 5´-TGTCAGAGAGACTGCAAGGATG-3´

SSD4:

FW:5´- TTGGCCATAGATATGGAGAATTGGA-3´ and RV:5´- GGCTCAAGAGTATTGCAGCAT-3´

SSD5:

FW:5´- GCTGGGAACAGAGTGGTGAA-3´ and RV:5´- GCTCCTCCCACCAAGAGTTC-3´

The following primers were used for RT-PCR and qRT-PCR:

Ubiquitin: FW: 5´-ATGTGAAGGCCAAGATCGGAG-3´ and RV: 5´-TAATAGCCACCCCTCAGACG-3´

GAPDH: FW: 5´-CCATGACAACTTTGGCATTG-3´ and RV: 5´-TCCCCACAGCCTTAGCAG-3´

DISP3: FW: 5´-CAGCAGTTTGACCTCTTCA-3´and RV: 5´-GCAACATCTGCAGGAAGGA-3´

Nestin: FW: 5´-AGGCTGAGAACTCTCGCTTGC-3´ and RV: 5´-GGTGCTGGTCCTCTGGTATCC-3´

βIII-tubulin: FW: 5´-TGGACAGTGTTCGGTCTGG-3´and RV: 5´-CCCTCCGTATAGTGCCCTTTG-3´

GFAP: FW: 5´-TGAGGCAGAAGCTCCAAGA-3´and RV: 5´-CCAGGGTGGCTTCATCTGC-3´

3.1.8 Immunostaining antibodies

Primary antibodies

DISP3: Rabbit polyclonal anti-DISP3 antibody, 1:400, obtained from M. Zikova, Ph.D.

GAPDH: Mouse monoclonal anti-GAPDH antibody, used as marker,1:2000,

GeneTex ref. GTX627408

Nestin: Monoclonal anti-nestin mouse antibody, clone rat-401, 1:400,

EMD Millipore ref. MAB353

β-III tubulin: Monoclonal mouse neuron-specific β-III tubulin antibody, 1:1000,

R&D Systems, ref. MAB1195

GFAP: Mouse monoclonal glial-specific anti-GFAP antibody, 1:400, Sigma-Aldrich ref. G3893

Secondary antibodies – immunoblotting

Anti-rabbit IgG, peroxidase-linked antibody, GE Healthcare ref. NA9340

Anti-mouse IgG, peroxidase-linked antibody, Cell Signaling Technology ref. 7076S

SuperSignal™ West Pico Chemiluminescent Substrate, Thermo Scientific ref. 34087

Secondary antibodies – immunofluorescence

Anti-Mouse IgG, Secondary Antibody, Alexa Fluor® 488:

Used for staining of mouse primary antibodies, visible in green, Invitrogen ref. A11029

Anti-Mouse IgG, Secondary Antibody, Alexa Fluor® 568:

Used for staining of primary mouse antibodies, visible in red, Invitrogen ref. A11031

Anti-Rabbit IgG, Secondary Antibody, Alexa Fluor® 488:

Used for staining of primary rabbit antibodies, visible in green, Invitrogen ref. A11034

Anti-Rabbit IgG, Secondary Antibody, Alexa Fluor® 568:

Used for staining of rabbit primary antibodies, visible in red, Invitrogen ref. A11036

3.1.9 Buffers and solutions

1xPBS: 150 mM NaCl, 1.5 mM KH2PO4, 2.7 mM Na2HPO4, pH 7.4

1xTAE: 40 mM Tris, 40 mM acetic acid, 1 mM EDTA, pH 8.0

Phenol-chloroform solution: 1:1 volumes; phenol equilibrated by 0.1 M Tris pH 8.0

Polyethylenimine (PEI): 1 mg/ml solution in water; sterilized by filtration through

0.22 µm filter.

1x Trypsin: 0.05 % trypsin, 0.02 % EDTA

TEG: 25 mM Tris pH 8.0, 10 mM EDTA pH 8.0, 50 mM glucose

Lysis buffer: 0.2 M NaOH, 2% SDS

Neutralization buffer: 3 M K+, 5 M Ac-

Phenol-chloroform solution: 1:1 of both volume; phenol equilibrated by 0.1 M Tris pH 8.0

1M Tris: 12.1 g of Tris base dissolved in 100 ml of deionized water

1 × Sample buffer (1x SB): 63 mM Tris HCl, 10% Glycerol, 2% SDS, pH 6.8

1× TGS buffer: 25 mM Tris, 192 mM glycine, 0.1% SDS, pH 8.3

1 × TG buffer: 25 mmol/l Tris, 192 mmol/l glycine, pH 8.3, buffer contained 20% methanol

1x TBS buffer: 50 mM Tris HCl, 150 mM NaCl, pH 7,5

1x TBST buffer: 1xTBS, 0,05% Tween-20

3.1.10 Proliferation assay materials

[methyl-3H]-Thymidine, Moravek Biochemicals and Radiochemicals ref. MT6034

MultiLex^{TM}A, Perkin Elmer ref. 1450-441

Filtermat A, Perkin Elmer ref. 1450-421

FilterMate Harvester, Perkin Elmer

Proliferation assays were evaluated by 1450 MicroBeta, Perkin Elmer.

3.1.11 Other materials

ProLong® Gold Antifade Mountant with DAPI, Life Techologies ref. P36941

Bovine Serum Albumin, Sigma-Aldrich ref. A2153

Triton X-1000, Serva ref. 39795

3.2 Methods

3.2.1 Nucleic acids work

Nucleic acid quantification

Concentration and quality of nucleic acids (both RNA and DNA) was measured by Nanodrop ND 1000.

Oligos annealing

1. Annealing mix (1µl of 100µM solution of both oligos, 1 µl of 10x NEB T4 Ligation Buffer, 6,5 µl of ddH_2O and 0,5 µl of NEB T4 PNK) was prepared.
2. The mix was incubated for 30 minutes at 37°C.

3. The mix was heated up to 95°C, then temperature ramped down to 25°C (5°C/minute).
4. Annealed oligos were diluted in nuclease free water in ratio 1:200 of oligos to water.

Restriction enzyme digestion

Conventional enzymes were used for digestion according to the protocol. Typically, 200-500 ng of plasmid DNA was used for digestion by 0,5 µl of enzyme in specific buffer. Reaction was stopped by heat inactivation at 95°C, or by addition of EDTA.

Agarose Gel Electrophoresis

Typically, it was used 0,8% - 1,5% (according to the fragment size) solution of agarose in TAE. Ethidium bromide (1:10000) was added and solution was gently mixed. Voltage was normally set up to maximally 9V/cm. Samples were mixed with 6x DNA Loading Dye (Thermo Scientific, ref. #R0611). DNA ladders were used according to the fragment size – 100bp DNA Ladder (BioLabs, ref. #N3231S) and Gene Ruler 1kb Plus (Thermo Scientific, ref. #R0611).

DNA extraction from agarose gel

QIAEX II Gel Extraction Kit

Reagents:

QIAEX II suspension: silica-gel particles

Buffer QX1: used for solubilization of agarose and binding of DNA to silica particles, it removes residual agarose

Buffer PE: removes salt contaminants

Procedure:

1. Desired DNA fragment was excised from the gel.
2. Three volumes of QG Buffer were added to 1 volume of gel fragment. The mix was incubated for 10 minutes at 50°C. The tube was eventually vortexed.
3. Isopropanol (1 volume of gel slice) was added and vortexed.
4. The gel solution was placed to the column. Column was centrifuged for 1 minute at 13 000 rpm (Eppendorf 5415R) and supernatant was discarded.
5. Column was washed with PE Buffer (750 µl).
6. DNA was eluted from the column by addition of nuclease free water (Ambion), water was eluted to the new tube by centrifugation.

T4 ligation

Normally, it was used 50 ng of backbone vector DNA and insert in 3:1 molar excess. Ligation was performed in 10 µl solution, with 1 µl of T4 Ligase (Fermentas) and 1 µl of 10x T4 Ligase Buffer (Fermentas). The ligation was performed at RT for 1 hour and whole amount of ligation mix was concomitantly used to transform 100 µl of competent cells.

pGEM subcloning

pGEM T Easy Vector System I

pGEM vector is pre-linearized plasmid with thymidine overhangs for easier subcloning of PCR product (polymerase adding adenine overhangs needs to be used).

Usually, for one reaction we used 50 ng of pGEM with 3:1 molar excess of PCR product. T4 ligase (1 µl, included) and 10x reaction buffer (1 µl, included) were added to 10µl reaction. Reaction mix was incubated for 16-18 hours at 4°C followed by 1 hour at RT. pGEM vector bears *lacZ* gene, that enables X-Gal blue/white selection, and T7 and SP6 sequencing primer sites.

Sequencing

Normally, we added 5 µl of 5µM solution of specific primers (see above) to 500 ng of plasmid DNA diluted in nuclease free water in total amount 10 µl. Sequencing was ordered from SEQme s.r.o. company and sequences were obtained in FASTA file.

Genomic DNA isolation

QIAamp® DNA Minikit

Reagents:

AL Buffer: used for cell lysis.

AW1 Washing Buffer: used to remove impurities from the DNA.

Proteinase K (20 mg/ ml): used to avoid protein contamination in isolated DNA.

Procedure:

1. The cells were harvested and resuspended in 200 µl of PBS, 20 µl of Proteinase K was added as well as 200 µl of AL Buffer.
2. The mixture was incubated at 56°C for 10 minutes and eventually vortexed.
3. Ethanol (200 µl, 96%) was added and tube was vortexed for 15 seconds.
4. The mix was placed into the column. It was centrifuged for 1 minute and 8 000 rpm (Eppendorf 5415R) and the supernatant was removed.
5. AW1 Washing Buffer (500 µl) was added and centrifuged for 3 minutes and 13 000 rpm.
6. The supernatant was removed and the column was centrifuged again for 1 minute and 13 000 rpm.
7. It was added 200 µl of nuclease free water to the column and incubated for 5 minutes at RT.
8. The column was centrifuged for 1 minute and 8 000 rpm – supernatant contained genomic DNA.

RNA isolation

1. The cells were lysed by Trizol Tri Reagent (BioTech, ref. TR118) and the lysate was incubated for 10 minutes at 4°C – 1ml of Tri Reagent per 3cm dish of cells.
2. The lysate was centrifuged for 10 minutes and 13 000 rpm (Eppendorf 5415R) and the supernatant was replaced to the new tube.
3. Chloroform (200 µl) was added and intensively vortexed for 30 seconds.
4. The mixture was incubated for 15 minutes at 4°C and then centrifuged for 15 minutes and 13 000 rpm.
5. Upper phase was transferred to the new tube and isopropanol (450 µl) was added.
6. The mixture was incubated for 16-18 hours at -20°C and centrifuged for 10 minutes and 13 000 rpm. The supernatant was removed.
7. The pellet was washed twice with 75% ethanol, centrifuged for 5 minutes and 13 000 rpm and the supernatant was removed.
8. The liquid was dried and pellet was resuspended in desired amount of nuclease free water.

DNase treatment

Whole procedure was performed at nuclease free conditions and at 4°C and all reagents were obtained from Promega.

Usually, RNA (1 µg) was diluted in nuclease free water in total volume of 8 µl. 10x DNase Buffer (1µl) and DNase (1 µl) were added. The reaction was incubated at 37°C for 30 minutes and stopped by addition of DNase Stop Solution and incubation at 65°C for 10 minutes.

Reverse transcription

Whole procedure was performed at nuclease free conditions and at 4°C. All the reagents were obtained from Promega.

1. RNA (1µg) was diluted in 14,5 µl of nuclease free water and 0,5 µl of Random Primers was added.
2. The mix was incubated at 70°C for 5 minutes and then at 4°C for 5 minutes.
3. RT premix (2,5 µl of 10x M-MLV RT Buffer, 1 µl of 12,5mM dNTP, 0,5 µl of RNasin and 5 µl of nuclease free water) was added to RNA solution.
4. M-MLV Reverse Transcriptase (1 µl) was added to the reaction.
5. The mixture was incubated for 1 hour at 37°C.
6. The reaction was stopped by incubation at 95°C for 2 minutes.

PCR – T7 Endonuclease assay, subcloning

PCR premix (1 µl of 4mM dNTP - Thermo Scientific, 0,5 µl of 10 mM FW primer, 0,5 µl of 10 mM RV primer,2 µl of 10x Taq Polymerase Buffer – BioLabs, and 0,3 µl of Taq Polymerase – BioLabs) was prepared. The template DNA (50 – 200 ng) was diluted in nuclease free water in total volume of 15,7 µl and the solution was mixed with PCR premix.

PCR cycle was performed in following conditions:

1. Initial denaturation was performed at 94°C for 3 minutes.
2. Cyclic denaturation was performed at 94°C for 30 seconds.
3. Primer annealing was performed according to specific primers. Normally, temperature varied in between 59-60°C for 50 seconds.
4. Extension was performed according to the length of amplified fragment – 1 minute of extension time per 1 kb of DNA fragment. Temperature was set up at 72°C.
5. Final extension step was performed at 72°C for 10 minutes.
6. At the end, temperature ramped down to 10°C.

Step 2 to 4 were repeated in cycle. Number of repeat varied in between 28 to 34.

PCR product phenol-chloroform extraction

This procedure was used for PCR product cleaning, mainly for T7 Endonuclease assay.

1. PCR product was diluted in water in total amount 225 µl.
2. NaAc solution (final concentration 0,5M) was added to PCR product and 250 µl of phenol/chloroform (1:1) mixture was added.
3. The mix was intensively vortexed and centrifuged for 3 minutes and 13 000 rpm (Eppendorf 5415R).
4. Upper phase was transferred to the new tube and 250 µl of chloroform was added.
5. The mixture was intensively vortexed and centrifuged for 3 minutes and 13 000 rpm.
6. The supernatant was transferred to the new tube and 250 µl of isopropanol was added.
7. The mixture was intensively vortexed and centrifuged for 10 minutes and 13 000 rpm, the supernatant was removed.
8. The pellet was washed by addition of 250 µl of 75% of ethanol. Centrifuged for 5 minutes and 13 000 rpm.
9. The supernatant was removed and the liquid was dried.
10. The pellet was resuspended in desired amount of nuclease free water.

qRT – PCR

For qRT-PCR procedure, the amount of RNA used for Reverse Transcription was 200 ng and Reverse Transcription product was diluted in nuclease free water in 1:1 ratio, this solution was then used as template for qRT-PCR reaction.

Reaction mix (2,5 µl of Light Cycler® SYBR Green Master, Roche, 1 µl of mix of 10mM FW and RV primers, 0,5 µl of nuclease free water and 1 µl of DNA template) was prepared.

The reaction was performed on Light Cycler®480 (Roche) and evaluated by its software.

PCR cycle was performed in following conditions:

1. Initial denaturation was performed at 95°C for 3 minutes.
2. Denaturation was performed at 95°C for 15 seconds.
3. Annealing of primers was performed at 61°C for 20 seconds.

4. Extension was performed at 72°C for 15 seconds.
5. Final extension was performed at 72°C for 3 minutes.
6. At the end, temperature ramped down to 4°C.

Steps 2 to 4 were repeated in 44 cycles.

T7 Endonuclease assay

Genomic DNA, isolated from the cells, was followed by PCR reaction and PCR product was cleaned up as described above. Primers were designed asymmetrically with respect to the CRISPR target site, to obtain bands with different size on gel electrophoresis after T7 endonuclease digestion.

1. DNA (200 ng) was diluted in nuclease free water and proper concentration of NEBuffer 2 (NEB) in total volume of 19 µl.
2. The mix was incubated at 95°C for 5 minutes and temperature then ramped down - from 95-85°C with rate 2°C per second, from 85-25°C with rate 0,1°C per second.
3. T7 Endonuclease (1 µl, NEB) was added to the mix and incubated for 20 minutes at 37°C.
4. The reaction was then stopped by addition of 0,25M EDTA (1,5 µl) and evaluated by agarose gel electrophoresis.

3.2.2 Bacterial work

X-Gal plates preparation

Mix: The mix (40 µl X-Gal, 100 µl 10mM IPTG and 100 µl LB) was equally spread to LB plate with antibiotics. White colonies were selected.

Transformation

1. Competent bacteria (100 µl) were thaw on the ice.
2. Ligation mix (5 µl) or plasmid DNA (1 µl) was added to the cells and gently mixed. The mix was incubated on the ice for 10 minutes.
3. Bacterial mix was incubated for 1 min at 42°C.
4. The mix was quickly cooled down and incubated for 10 minutes on the ice.
5. LB medium (750 ml) was added and the whole mix was incubated for 45 minutes at 37°C and constantly shaking for 270 rpm.
6. The tube was centrifuged for 5 min and 6500 rpm (Eppendorf centrifuge 5415 R).
7. Supernatant was removed and the pellet was resuspended in the fresh LB medium (100 µl).
8. Bacteria were spread on the plate containing antibiotics according to the plasmid resistance. Plates were cultivated at 37°C for 12-18 hours.

Plasmid DNA isolation:

"Miniprep" isolation

1. Desired colonies from LB plate were picked up and cultivated in 2 ml of LB medium with antibiotic according to the plasmid resistance – at 37°C and 270 rpm for 16-18 hours.
2. The culture was centrifuged for 5 minutes and 13 000 rpm.
3. The pellet was resuspended in 50 µl of TEG buffer.
4. Lysis buffer (50 µl) was added to the bacterial mixture and the mix was incubated at room temperature (RT) for 5 minutes.
5. Neutralisation buffer (50 µl) was added and the tube was vortexed.
6. Phenol/chloroform solution (150 µl) was added and the tube was vortexed intensively.
7. The sample was centrifuged for 5 minutes and 13 000 rpm.
8. Upper phase (125 µl) was replaced to the new tube and isopropanol (125 µl) was added. The tube was vortexed intensively.

9. The sample was centrifuged for 10 minutes and 13 000 rpm.
10. Supernatant was removed and 500 µl of 75% ethanol was added.
11. The sample was centrifuged for 5 minutes and 13 000 rpm.
12. Supernatant was removed and the pellet was dried.
13. The pellet was resuspended in nuclease free water (Ambion).

"Midiprep" isolation

JetStar® 2.0 Plasmid Purification Kit

Reagents:

Cell resuspending buffer (E1): 50 mM Tris-HCl, pH 8.0, 10 mM EDTA, RNase A in final concentration 100 µg/ml

Lysis buffer (E2): 0.2 M NaOH, 1% (w/v) SDS

Precipitation buffer (E3): 3.1 M Potassium acetate, pH 5.5

Equilibration buffer (E4): 0.1 M Sodium acetate, pH 5.0, 0.6 M NaCl, 0.15% (v/v) TritonX-100

Wash buffer (E5): 0.1 M Sodium acetate, pH 5.0, 0.8 M NaCl

Elution buffer (E6): 0.1 M Tris-HCl, pH 8.5, 1.25 M NaCl

RNase A: 20 mg/mL in 50 mM Tris-HCl, 10 mM EDTA, pH 8.0

Procedure:

1. E4 buffer (10 ml) was added and let drain by gravity flow to equilibrate the column.
2. Overnight bacterial culture (50 ml) was centrifuged for 5000 g and 10 minutes and the supernatant was removed.
3. The pellet was resuspended in the E1 buffer (4 ml), until the mixture was homogenous.

4. E2 buffer (4 ml) was added, gently mixed until it was homogenous and incubated for 5 minutes at RT.
5. E3 buffer (4 ml) was added, gently mixed until it was homogenous and centrifuged for 5000 g for 30 minutes.
6. The supernatant was loaded to the equilibrated column and let drain by gravity flow.
7. Column was washed twice with E5 buffer (10 ml). Buffer was let to drain by gravity flow.
8. The column was replaced to clean tube and E6 buffer (5 ml) was added and let drain by gravity flow.
9. Isopropanol (3,5 ml) was added and the mixture was mixed. It was centrifuged for 5000 g and 30 minutes at 17°C.
10. The supernatant was removed and the pellet was resuspended in 1 ml of 75% ethanol until it was homogenous. The whole mixture was replaced to 1,5ml tube.
11. The sample was centrifuged for 5 minutes and 13 000 rpm (Eppendorf 5415 R).
12. The supernatant was removed and the pellet was dried. Afterwards, it was resuspended in 50 µl of nuclease free water (Ambion).

3.2.3 Eukaryotic cell work

Adherent cell lines cultivation

All of the cell lines were cultured in 5% carbon dioxide atmosphere at 37°C.

HEK Phoenix-Eco, HEK 293 FT, DAOY and C 17.2 cells were cultured adherently on the dish (TPP) with 60-90 % of confluency. Cells were subcultured every second-third day.

Adherent cell lines subculturing

1. Culture medium was removed from the dish.
2. Cells were washed with PBS buffer.
3. Trypsin solution was added to cells and cells were incubated for 5 minutes at 37°C.
4. Cell suspension in trypsin solution was replaced to the tube and adequate volume of growing media was added.

5. The tube was centrifuged for 3 minutes at 120 g.
6. Supernatant was discarded and the pellet was resuspended in desired amount of fresh medium.
7. Cell suspension was transferred onto new plastic dish.

Spheroid cell line cultivation

D341 cells were cultured in 5% carbon dioxide atmosphere at 37°C in spheroid suspension in cultivation flask (Greiner). Cells were subcultured every second-third day.

Spheroid cells subculturing

1. Cell suspension was collected into the tube.
2. Adherent subpopulation of cells was washed with PBS (1x). Cells in PBS were transferred into the tube.
3. Trypsin solution was added and cells were incubated at 37°C for 5 minutes.
4. Cell suspension in trypsin solution was transferred to the tube.
5. The tube was centrifuged for 3 minutes and 120 g.
6. Supernatant was discarded and pellet was resuspended in desired amount of growing medium.
7. Cell suspension was transferred into new flask.

C 17.2 cells differentiation

1. Cells were seeded with 50% confluency on the dish.
2. Next day (day 0) the growing medium was changed for differentiating medium.
3. Day 3 change of medium for fresh differentiating medium.
4. Day 7 end of differentiation.

Lipofectamine transfection

1. Cells were seeded day before to be 90% confluent in the day of transfection, 10cm dish size was normally used for transfection.
2. Mix of 500 µl of Opti-MEM and 10 µg of plasmid DNA was prepared.
3. Mix of 480 µl of Opti-MEM and 20 µl of Lipofectamine was prepared.
4. Both mixtures were incubated for 5 minutes at RT and gently mixed continuously.
5. Lipofectamine/Opti-MEM and DNA/Opti-MEM mixtures were mixed together and incubated for 20 minutes at RT and gently mixed continuously.
6. The culture medium was changed for fresh medium without P/S antibiotic content.
7. The transfection mixture (Opti-MEM, Lipofectamine and DNA) was added to the cells.
8. Cells were incubated at 37°C for 24 hours.
9. The medium was change for fresh growing medium (with P/S). Optionally, selective antibiotics were added.

PEI transfection

1. Cells were seeded day before to be 60-70% confluent in the day of transfection, 10cm dish size was normally used for transfection.
2. Mix of 825 µl of sodium chloride water solution (150 mM) and 20 µg of DNA was prepared.
3. Mix of 725 µl of sodium chloride water solution (150 mM) was mixed with 100 µl of PEI.
4. Both mixtures were vortexed and incubated for 15 minutes at RT.
5. Sodium chloride solution/PEI and sodium chloride solution/DNA mixtures were mixed together, vortexed and incubated for 10 minutes at RT.
6. The culture medium was changed for only DMEM.
7. The transfection mixture (sodium chloride solution, PEI and DNA) was added to cells.
8. The cells were incubated for 2,5 hours at 37°C.
9. The medium was changed for fresh DMEM. The cells were incubated for 3 hours at 37°C.

10. The medium was changed for fresh growing medium without P/S antibiotic content.

Retroviral transduction

1. HEK Phoenix-Eco cells (10cm Petri dish) were used for retrovirus production – cells were transfected by Lipofectamine method with pBabe constructs (day 0).
2. Day 2, culture medium of HEK cells was collected and centrifuged for 30 minutes and 3800 g.
3. The supernatant was transferred to the new tube and centrifuged for 30 minutes and 3800 g.
4. The supernatant was mixed with 4µg/ml of polybrene (Millipore, ref. TR-1003-G) and HS (to final concentration 5%) and was added to the final cells (10cm dish).
5. The cells were incubated for 6 hours at 37°C.
6. The culture medium was changed for fresh growing medium.
7. The cells were incubated for 24 hours at 37°C.
8. Specific dose of selective antibiotic was added.

Lentiviral transduction

1. HEK 293 RT cells (10cm Petri dish) were used for lentiviral production. Cells were co-transfected by PEI method with pCMV-VSV-G, psPAX2 and pLentiCRISPR plasmids in ratio 1:1,5:2 in final of 20 µg of DNA (day 0).
2. Day 2, culture medium was collected and centrifuged for 15 minutes and 3800 g.
3. The supernatant was replaced to the new tube and PEG-it (SBI, ref. LV810A-1) was added to the final ratio 1:5.
4. The mixture was incubated at 4°C for 16-18 hours, gently shaking constantly.
5. The mixture was centrifuged for 30 minutes and 3800 g and the supernatant was discarded.
6. The pellet was resuspended in 1 ml of PBS.
7. Transduction mix (500 µl of viral solution with 500 µl of growing media) was added to the final cells (3cm dish).

8. The cells were incubated for 24 hours at 37°C.
9. Culture medium was changed for fresh growing medium.
10. The cells were incubated for 24 hours at 37°C.
11. Specific dose of selective antibiotic was added.

Cell fixation

1. Culture medium was removed from the cells.
2. The cells were washed with PBS.
3. Paraformaldehyde (4%) was added to the cells and it was incubated for 15 minutes at 4°C.
4. The cells were washed 3 times for 5 minutes with PBS at RT.
5. Optionally stored in PBS at 4°C.

Antibody staining

1. Fixed cells were permeabilized by 0,1% Triton X-100 in PBS for 15 minutes at RT.
2. The cells were washed 3 times for 5 minutes with PBS at RT.
3. The blocking solution containing 2% NGS and 1% BSA in PBS was prepared and added to the cells. It was incubated for 1 hour at RT.
4. Primary antibody (in specific concentration) was diluted in 1% BSA in PBS and was added to the cells. It was incubated for 16-18 hours at 4°C.
5. The cells were washed 3 times for 5 minutes with PBS at RT.
6. Secondary antibody (1:1000) was diluted in 1% BSA solution in PBS (1x) and was added to the cells. It was incubated for 1 hour at RT – kept in dark.
7. The cells were washed 3 times for 5 minutes with PBS at RT.
8. The cells were mounted with ProLong reagent containing DAPI.

Thymidine incorporation assay

1. Cells were seeded into 96 well plate in three different concentrations and ^{3}H-Thymidine was added (8,54 ng in 125 µl of growing medium).
2. The cells were cultivated for 8 hours at 37°C and then quickly frozen in -80°C.
3. The cells were thawed and cell lysate was transferred to Printed Filtermat A membrane by Filtermat Harvester, the liquid was dried.
4. MultiLex A gel was melted on the membrane and cooled down.
5. The amount of incorporated ^{3}H-Thymidine in the membrane was measured by 1450 MicroBeta.

Cell cycle measurement

1. The cells were collected and centrifuged for 3 minutes and 120 g. The supernatant was removed.
2. The cells were washed with PBS, centrifuged for 3 minutes and 120 g. The supernatant was removed.
3. Single cell suspension was made in 0,5 ml of PBS.
4. The cell suspension in PBS was slowly added to 4,5 ml of 70% ethanol at 4°C.
5. The cell suspension was incubated at -20°C for 16-18 hours.
6. The cell suspension was centrifuged for 7 minutes and 3800 g and the supernatant was removed.
7. The cells were washed twice with PBS and centrifuged for 7 minutes and 3800 g, the supernatant was removed.
8. Single cell suspension was made in 0,1 ml of PBS.
9. Staining mix (90 µl of PBS 1x, 2 µl of 10% Triton X-1000, 4 µl of RNAse A, 10 mg/ml, and 4 µl of propidium iodid, 1 mg/ml) was prepared and added to the cell suspension.
10. The cell suspension was incubated for 15 minutes at 37°C.
11. The cell cycle was measured by LSR II flow cytometer (BD Biosciences) and data were evaluated by FlowJo 8.8.6 software.

3.2.4 Protein work

Protein isolation

1. The cells were dispersed into 1 ml of PBS, centrifuged for 3 minutes and 2500 rpm (Eppendorf 5415R) and the supernatant was removed.
2. The pellet was resuspended in 200 µl of SB buffer and incubated for 5 minutes at 95°C.
3. The mixture was twice sonicated for 20 seconds.
4. The mix was centrifuged for 5 minutes and 13 000 rpm.
5. The bromphenol blue dye was added and sample was used for SDS-PAGE, eventually stored at -80°C.

SDS-PAGE

Precast gradient 4-15% polyacrylamide gel (Biorad) were used for protein separation. The protein samples were loaded on the gel and 1x TGS buffer was used as running buffer. Samples ran at 25 mA per gel.

Western blotting

Separated protein samples were transferred to the nitrocellulose membrane. As running buffer, 1x TG buffer was used and 100 V were set up for 1 hour. The blotting buffer was cooled down during whole procedure by addition of ice bucket.

Immunostaining of western blot

1. The membrane was first blocked by 5% non-fat milk solution in TBST buffer for 20 minutes.
2. The membrane was washed with TBST.

3. Primary antibody was diluted in 1% non-fat milk solution in TBST buffer and added to the membrane and incubated for 16-18 hours at RT.
4. The membrane was washed with TBST.
5. Secondary antibody was added and incubated for 2 hours.
6. The membrane was washed with TBST.
7. ECL reagents (in 1:1 ratio of volume) were added to the membrane, incubated for 3 minutes.
8. The membrane was exposed to medical X-ray film and developed by Kodak developing machine.

3.2.5 Statistical analysis

Paired t-test was used to analyse statistics of selected experiments. All analysis was performed by GraphPad Prism® 5.0c. Asterisks in graphs indicate: * $P < 0,05$, ** $P < 0,01$, *** $P < 0,001$.

4. Results

4. 1 DISP3 overexpression

First, we started to ask for cell line suitable for both DISP3 overexpression and knock-out experiments. As DISP3 is expressed mainly in the neural tissue and the retina, we chose several human cell lines of neural and retinal origin, which we had in our depository. D341, D425 and DAOY medulloblastoma cell lines were chosen as well as Y79 retinoblastoma cell line. Moreover, we also decided to look for DISP3 expression in MCF-7, breast cancer cell line. As a control for normalization we used HEK 293 cells. We performed qRT-PCR to measure *DISP3* expression on mRNA level (Figure 4.1).

We showed, that expression in distinct medulloblastoma cell lines varied. D341 and D425 cell lines reveal increased *DISP3* expression compared to HEK cells, when *DISP3* expression in DAOY cells was low. Retinoblastoma cell line, Y79, showed enormous increase in *DISP3* expression, when compared to HEK cells. Finally, breast cancer MCF-7 cells showed very low expression (Figure 4.1).

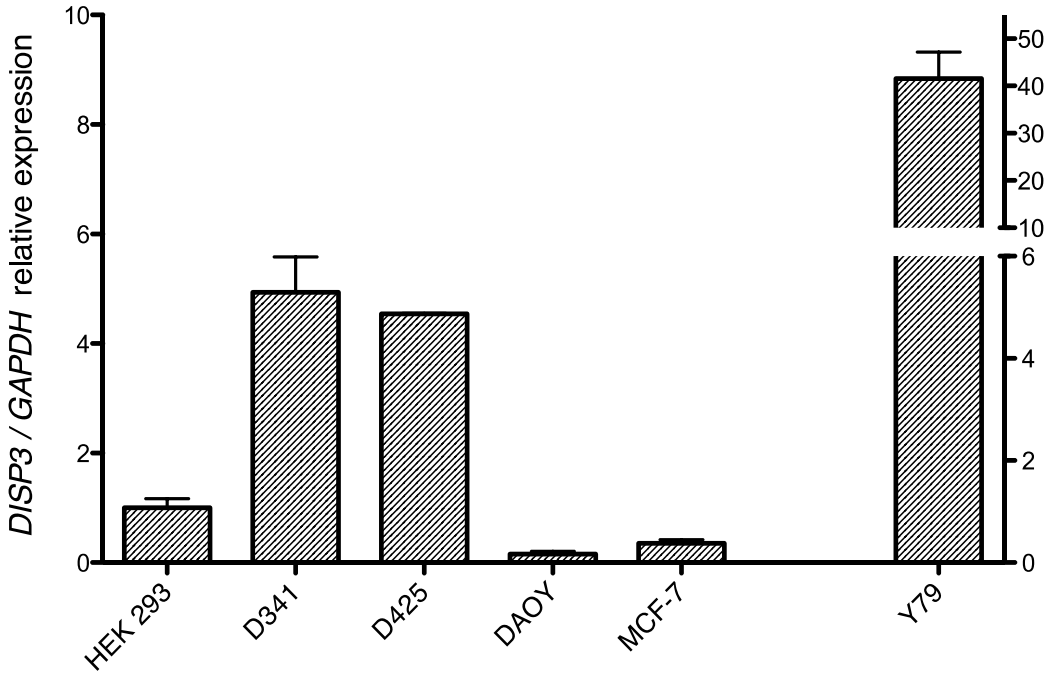

Figure 4.1. The graph shows *DISP3* expresion in D341, D425, DAOY, HEK293, MCF-7 and Y79 cell lines analysed by qRT-PCR. The data were normalized to HEK293 cell line. Error bars represents standard deviation of three independent experiments.

Distinct medulloblastoma cell lines reveal different level of *DISP3* expression, which makes them suitable for overexpression and knock-out studies. We decided to use DAOY cells, with low expression of DISP3 for over-expression studies and D341 cell line with significantly increased level of DISP3 expression for knock-out experiments.

We transfected DAOY cells with pCDNA3 – DISP3 construct expressing human DISP3 and as a control we used empty pCDNA3 vector. After transfection, we selected DAOY cells by addition of G418. *DISP3* expression was concomitantly proved by RT-PCR (Figure 4.2).

When we obtained pCDNA3 and pCDNA3 – DISP3 stable cell cultures, we performed ^{3}H-Thymidine incorporation assay to analyse effect of DISP3 overexpression on proliferation of DAOY cells (Figure 4.3). Cells ectopically expressing DISP3 reveals almost 2-fold increased proliferation compared to control cells. These data shows, that DISP3 ectopic expression promotes DAOY cells proliferation.

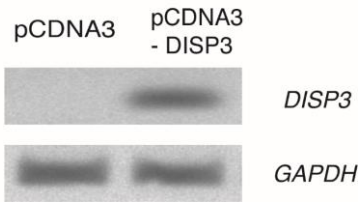

Figure 4.2. The picture shows *DISP3* expression in DAOY cells transfecetd with pCDNA3-DISP3 construct, cells with empty pCDNA3 vector are used as a control. Expression was analysed by RT-PCR and GAPDH was used as a loading control.

It was shown that distinct subtype of medulloblastoma may arise within neural progenitor subpopulation (Schuller, Heine et al. 2008, Yang, Ellis et al. 2008). Moreover, medulloblastoma tumors contain cells with stem cell properties still capable to differentiate (Hemmati, Nakano et al. 2003). Based on these findings, we asked, whether DISP3 expression may also affect cell differentiation. Here, we use mouse neural progenitor cell line C 17.2, derived from the cerebellum (Snyder, Deitcher et al. 1992), which was shown to be capable of differentiation to neurons and astrocytes (Lundqvist, El Andaloussi-Lilja et al. 2013), to study the impact of overexpression of DISP3 on cell differentiation.

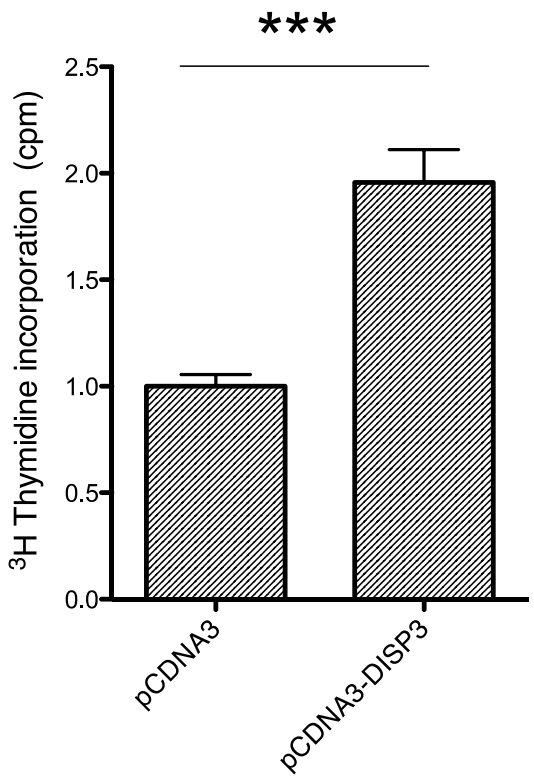

Figure 4.3. The graph shows ^{3}H-Thymidine incorporation in DAOY pCDNA3 and pCDNA3-DISP3 transfecetd cells. The data were normalized to pCDNA3 transfected cells. Error bars represents standard deviation.

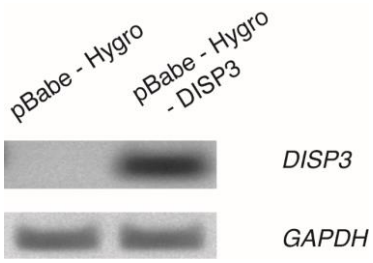

Figure 4.4. The picture shows *DISP3* expression in pBabe-Hygro and pBabe-Hygro-DISP3 transduced C 17.2 cells. Expression was analysed by RT-PCR and GAPDH was used as a loading control.

We generated C 17.2 with DISP3 ectopic expression by retroviral transduction of pBabe – Hygro – DISP3 construct, empty pBabe – DISP3 vector was used as a control. We added hygromycin to obtain DISP3 stably expressing cells and confirmed the expression by RT – PCR (Figure 4.4), immunoblotting (Figure 4.5) and by immunofluorescence (Figure 4.6).

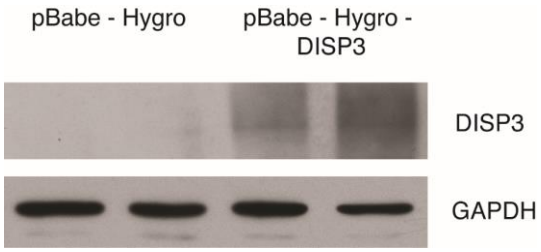

Figure 4.5. The picture shows DISP3 expression in pBabe-Hygro and pBabe-Hygro-DISP3 transduced C 17.2 cells. Expression was analysed by western blotting and GAPDH was used as a loading control.

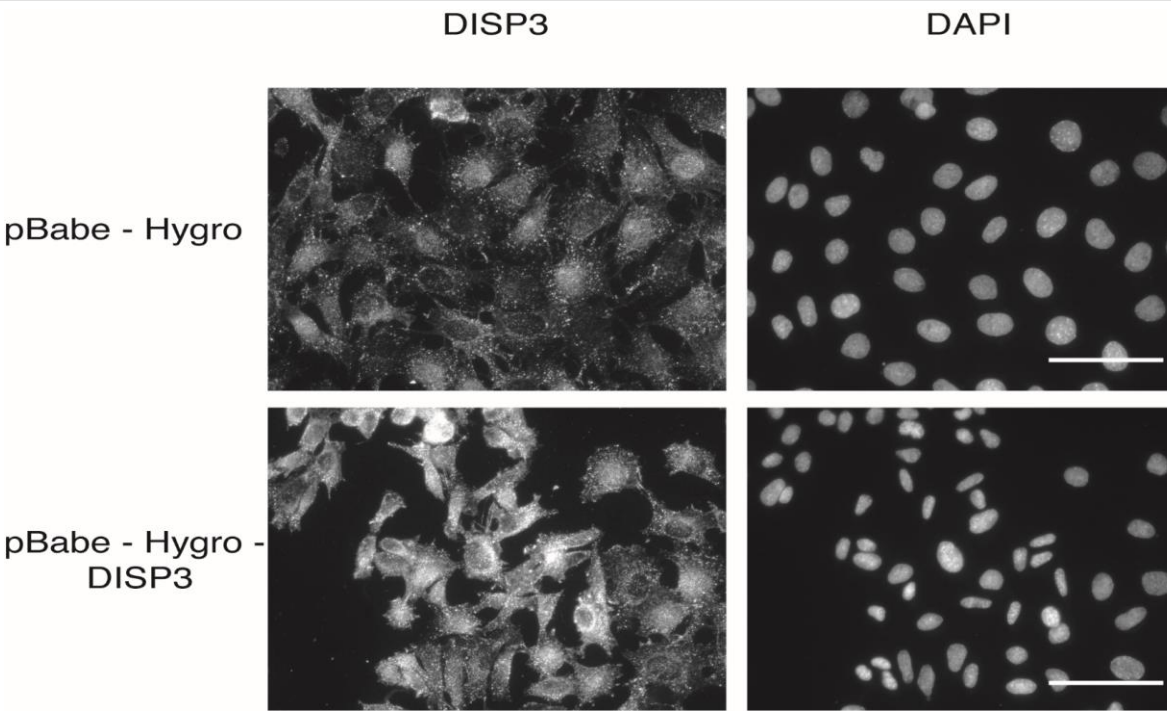

Figure 4.6. The picture shows immunofluorescence staining of pBabe-Hygro and pBabe-Hygro-DISP3 transduced C 17.2 cells with DISP3 antibody. DAPI staining was used for visualization of cell nuclei. Bar indicates 50 µm.

With pBabe – Hygro – DISP3 stable C 17.2 cells we performed ^{3}H – Thymidine incorporation assay to measure DISP3 effect on the proliferation as well as we did with DAOY cell line. DISP3 ectopically expressing C 17.2 cells revealed 1.7 – fold increased proliferation compared to control cells (Figure 4.7). This proves the result we obtained with DAOY cells.

Next, we performed differentiation experiment with C 17.2 cells transduced by pBabe – Hygro - DISP3 construct, as a control we used an empty vector. We differentiated C 17.2 cells according to protocol of Lundqvist et. al. (Lundqvist, El Andaloussi-Lilja et al. 2013). Under these conditions, C 17.2 cells are capable of differentiation into mixed population of neurons and astrocytes within 7 days, when cultured with N2 supplement, BDNF and NGF.

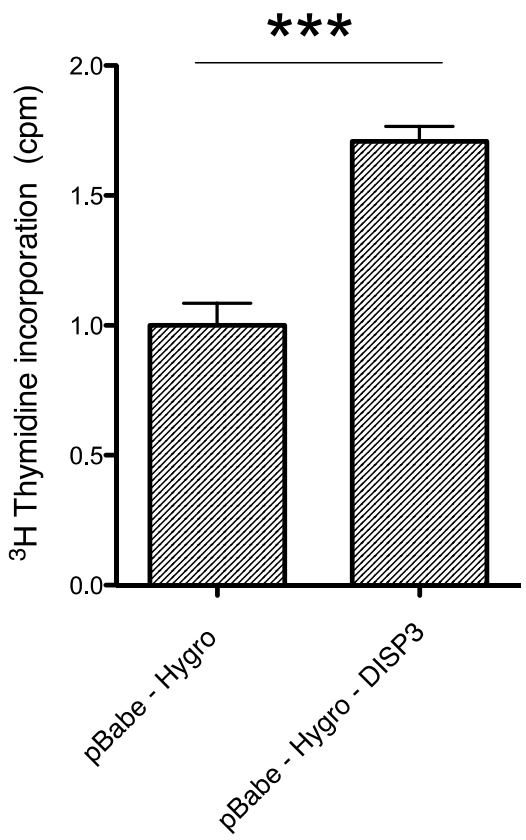

Figure 4.7. The graph shows ^{3}H-Thymidine incorporation in pBabe-Hygro and pBabe-Hygro-DISP3 transduced C 17.2 cells. The data were normalized to pBabe-Hygro transduced cells. Error bars represents standard deviation.

Upon differentiation conditions we observed morphological changes in both DISP3 expressing and control cells. While C 17.2 cells cultured under growing conditions showed polygonal morphology, differentiated cells showed neuron-like protrusions.

In control cells, we observed first protruded shapes at the day 5 of treatment and at the day 7 cells showed final differentiated shape. C 17.2 cells with DISP3 ectopic expression showed different behaviour compared to control cells. At the day 5 of treatment, they showed only slightly protruded shape, at the day 7 most of cells were protruded, however, neuron-like shape was not observed (Figure 4.8). These data show that cells with DISP3 ectopic expression undergo morphological changes later than controls.

To analyse differentiation of C 17.2 cells, we collected cell samples at the day 0, 1, 2, 3, 5 and 7 of differentiation and performed qRT-PCR (Figure 4.9a, b, c) and immunofluorescence microscopy (Figure 4.10, 4.11 and 4.12) of cell subtype specific markers. We used Nestin as a marker of neural progenitor, βIII-tubulin as a marker of neuronal and GFAP as a marker of astrocytic differentiation.

Upon differentiation conditions, we observed expected decrease of Nestin mRNA in both control and DISP3 ectopically expressing cells, as cells were losing their progenitor properties. At the day 1 and 2 of differentiation, cells ectopically expressing DISP3 revealed significantly higher level of Nestin mRNA, which was not observed at the day 3 or later (Figure 4.9a). We also stained our cells with Nestin specific antibody to observe this marker on protein level. Expression of Nestin protein was high in both DISP3 expressing and control cells, however, at the day 2 of differentiation, DISP3 expressing cells showed significant increase in Nestin antibody staining compared to control (Figure 4.10).

Next, we observed huge variations of *βIII-tubulin* mRNA levels during differentiation period. The main increase of *βIII-tubulin* expression was observed between days 2 – 5, and then the expression slightly decreased. However, during all the differentiation period, we observed significantly lower level of *βIII-tubulin* mRNA expression in DISP3 expressing cells compared to control (Figure 4.9b). When we performed βIII-tubulin antibody staining, cells with DISP3 ectopic expression revealed less staining than control already at the initial day of differentiation. At the day 7, cells ectopically expressing DISP3 showed significantly less βIII-tubulin than control cells. Also, βIII-tubulin positive cells in both cultures showed huge

difference in morphology. In control cells, they revealed neuron – like shape. This result was not observed, when cells expressed DISP3 (Figure 4.11).

Finally, we analysed GFAP expression. At the initial day of differentiation, both DISP3 expressing and control cells showed very low GFAP expression on qRT – PCR, while after 3 days of treatment expression was rapidly increasing until the end of differentiation. GFAP expression in DISP3 expressing cells remained lower during the whole differentiation period compared to control cells (Figure 4.9c).

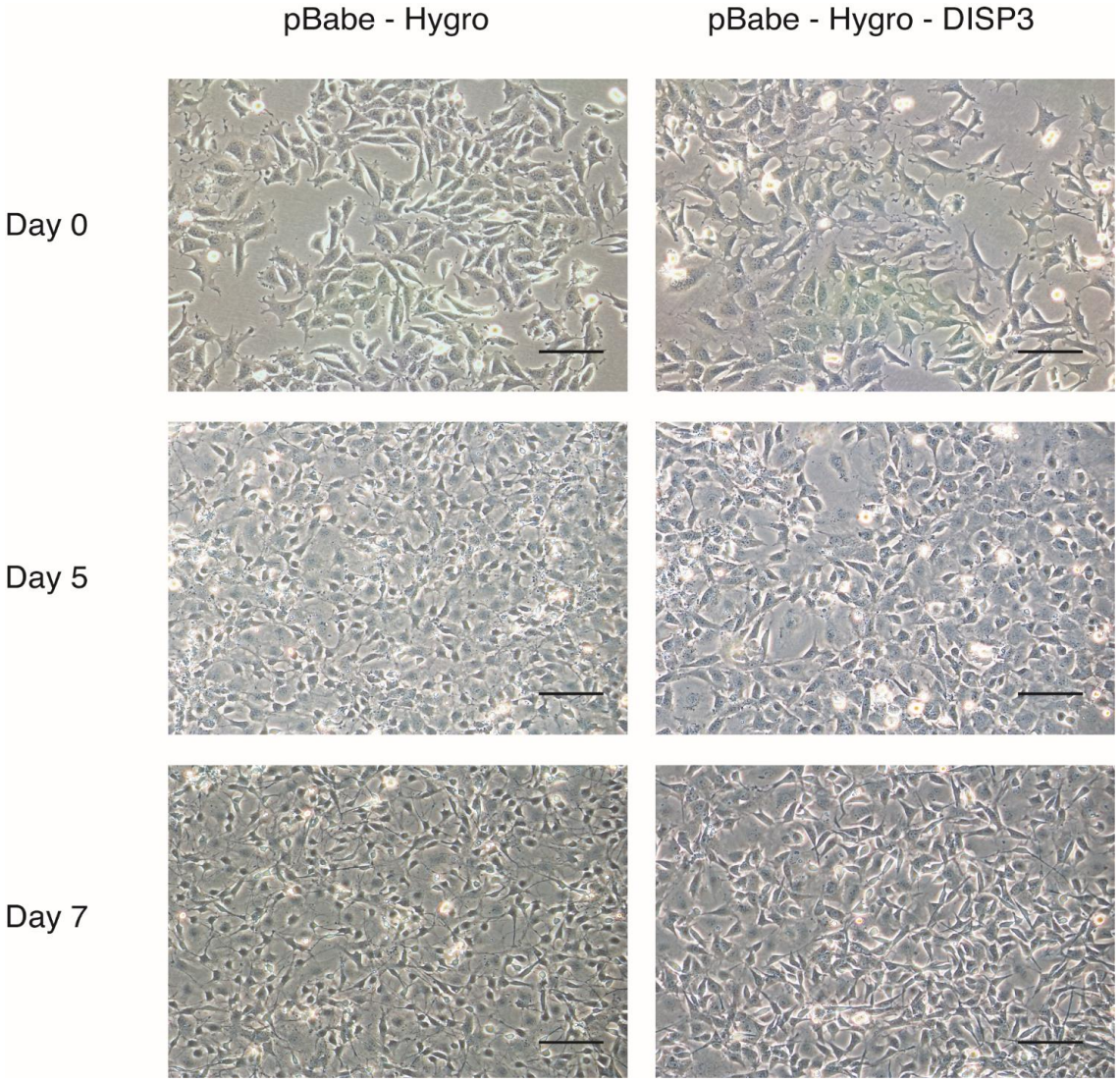

Figure 4.8. The picture shows pBabe-Hygro and pBabe-Hygro-DISP3 transduced C 17.2 cells upon differentiation conditions. Bar indicates 100 µm.

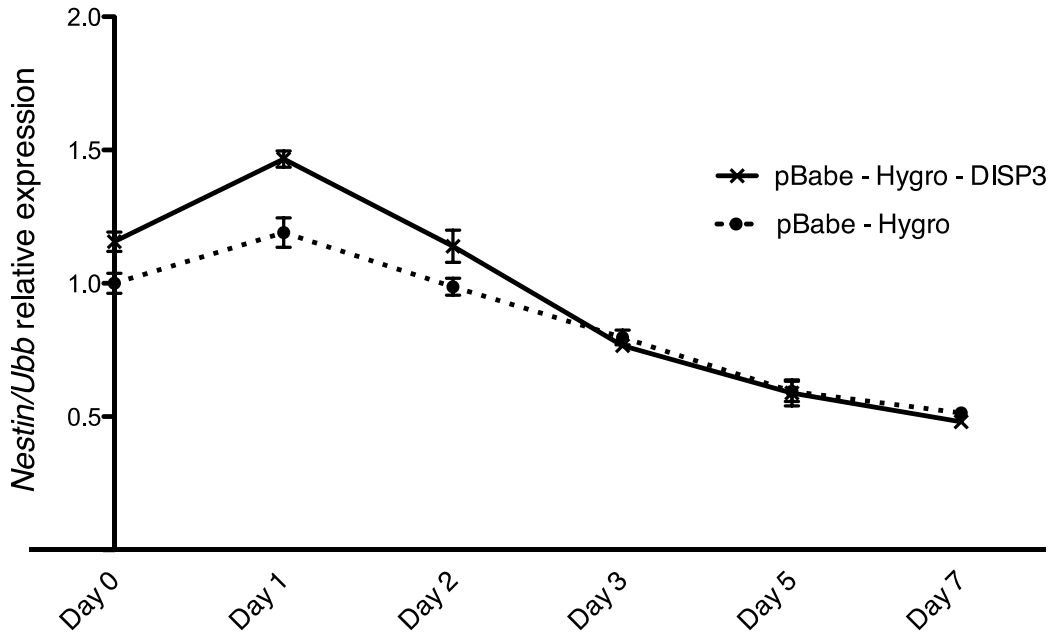

Figure 4.9a. The graph shows expression of *Nestin* markers. The expression was analysed by qRT-PCR and normalized to pBabe-Hygro C 17.2 cells. Error bars represent standard deviation.

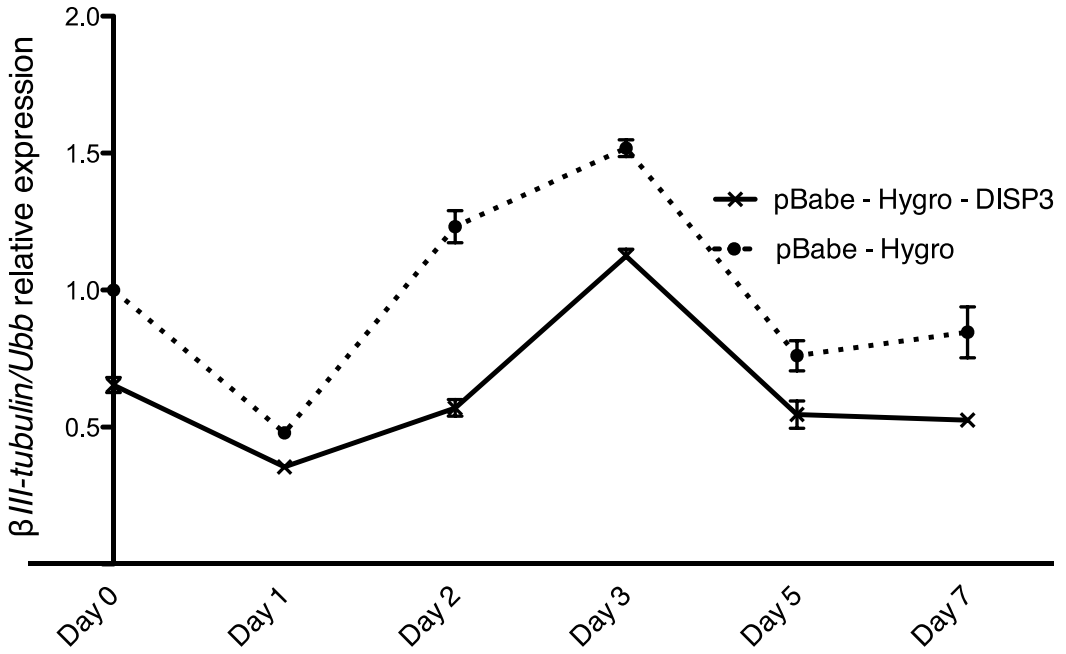

Figure 4.9b. The graph shows the expression of *βIII-tubulin* marker. The expression was analysed by qRT-PCR and normalized to pBabe-Hygro C 17.2 cells. Error bars represent standard deviation.

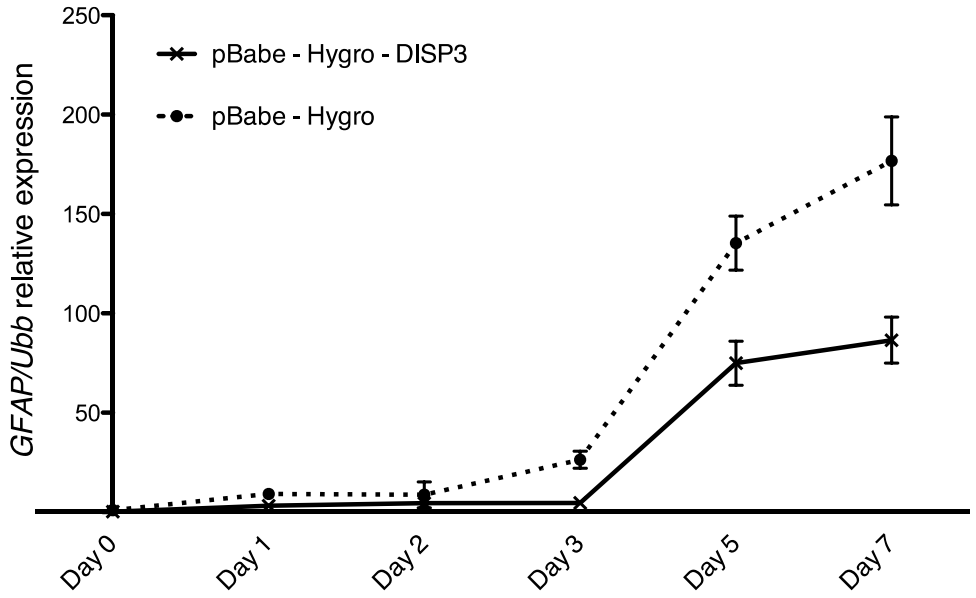

Figure 4.9c. The graph shows expression of *GFAP* marker. The expression was analysed by qRT-PCR and normalized to pBabe-Hygro C 17.2 cells. Error bars represent standard deviation.

These results were consistent with GFAP specific antibody staining where we observed very low expression of GFAP in both DISP3 expressing and control cells at the day 0. After 7 days of differentiation, GFAP protein level increased while it was significantly lower in DISP3 ectopically expressing cells compared to control (Figure 4.12).

All the data show that ectopic DISP3 expression promotes delay in C 17.2 cell differentiation as it is apparent on neuronal and astrocytic marker levels as well as on morphological changes. Both GFAP and βIII-tubulin reveal lower expression in DISP3 expressing cells while Nestin, as a marker of neural progenitor, reveals higher expression in the initiation of differentiation process. Together with higher proliferative rate of DISP3 expressing C 17.2 and DAOY cells, our experiments suggest DISP3 role in regulation of cell fate decision within cells of neural origin.

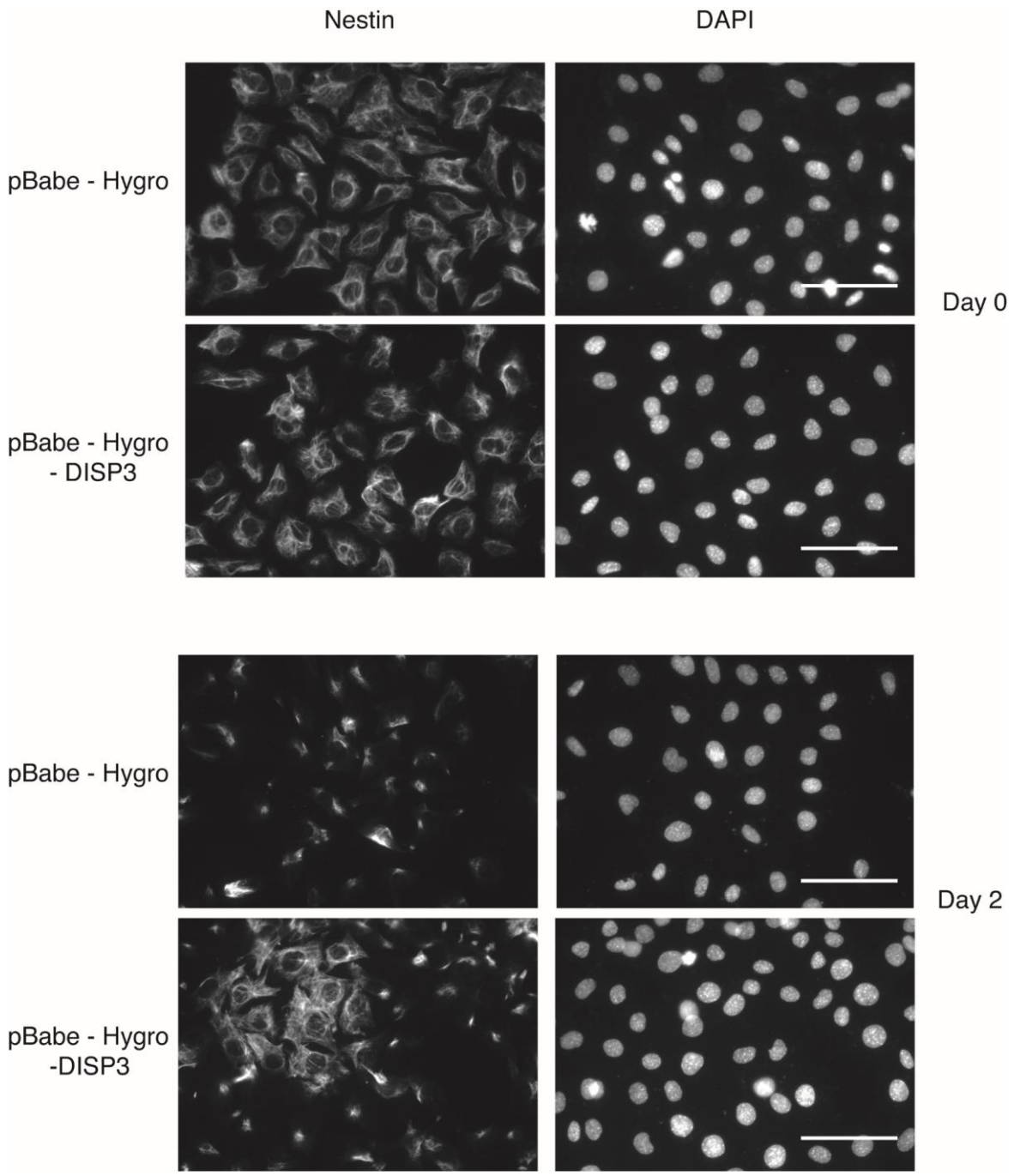

Figure 4.10. The picture shows immunofluorescence staining of pBabe-Hygro and pBabe-Hygro-DISP3 transduced C 17.2 cells with Nestin antibody. DAPI staining was used for visualisation of cell nuclei. Bar indicates 50 µm.

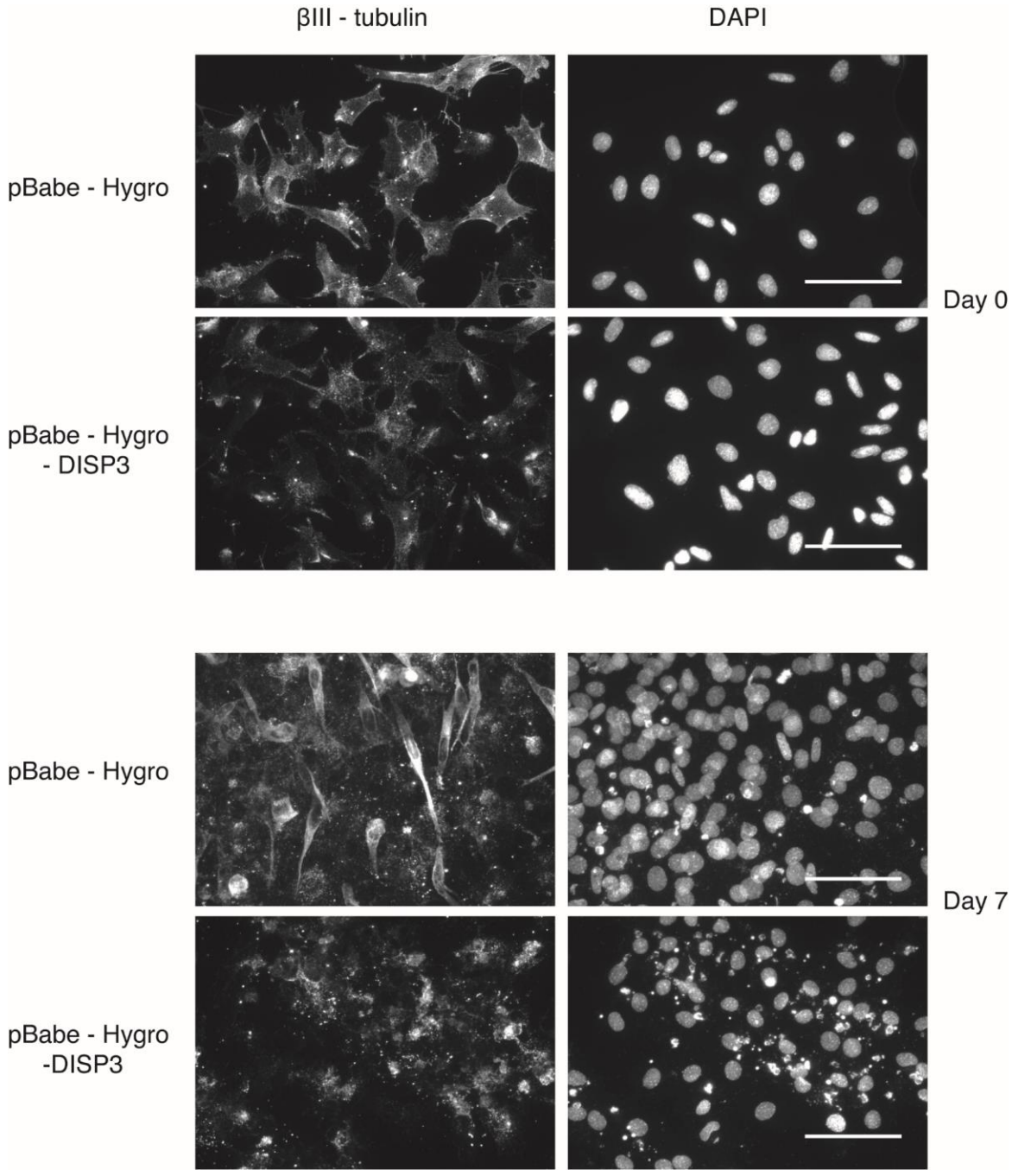

Figure 4.11. The picture shows immunifluorescence staining of pBabe-Hygro and pBabe-Hygro-DISP3 transduced C 17.2 cells again βIII-tubulin protein. DAPI staining was used for visualization of cell nuclei. Bar indicates 50 µm.

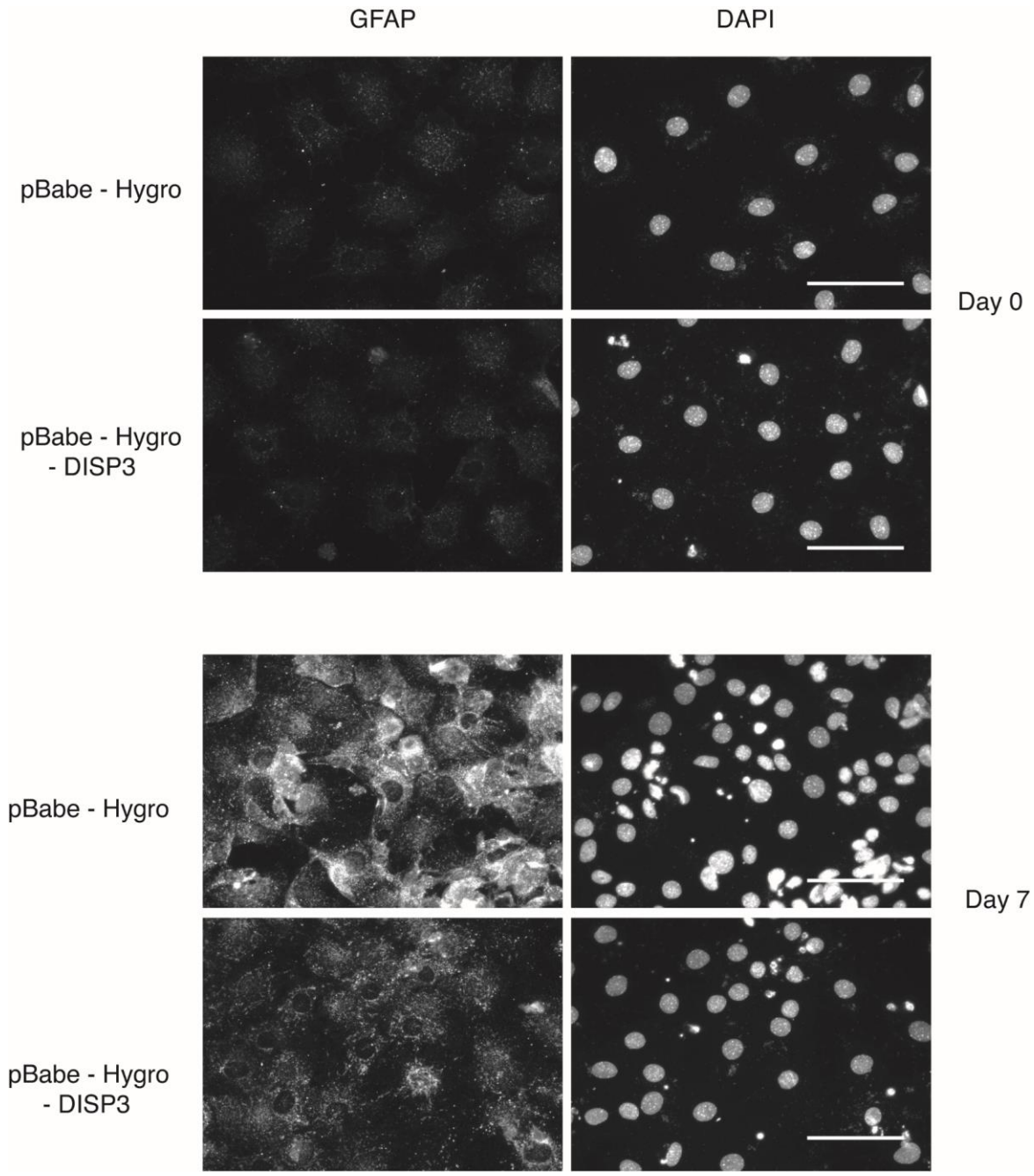

Figure 4.12. The picture shows immunofluorescnece staining of pBabe-Hygro and pBabe-Hygro-DISP3 transduced C 17.2 cells with GFAP antibody. DAPI staining was used for visualization of cell nuclei. Bar indicates 50 µm.

4.2 DISP3 targeting

Next, we wanted to analyse whether lack of DISP3 expression has effect on cell proliferation. For this purpose, we decided to use D341 cells as we showed that *DISP3* expression is high in this cell line (Figure 4.1). Moreover, these cells have human medulloblastoma origin same as DAOY cells, which we used for the overexpression experiment.

First, we chose CRISPR target sequences in *DISP3* gene to mutate six different sites. All the sites were targeted into exons of the gene – Loop 1.1, Loop 1.2 and Loop 1.3 target sites were found in the second exon, Loop 1.4 target site was found in the third exon, SSD4 target site was found in the fourth exon and finally SSD5 target site was found in the fifth exon. All the sites of predicted mutations lay within the first third of *DISP3* transcript and were chosen with the respect to the protein structure - Loop CRISPR sites target first luminal loop of DISP3 and SSD CRISPR sites target SSD domain of DISP3 protein (Figure 4.13).

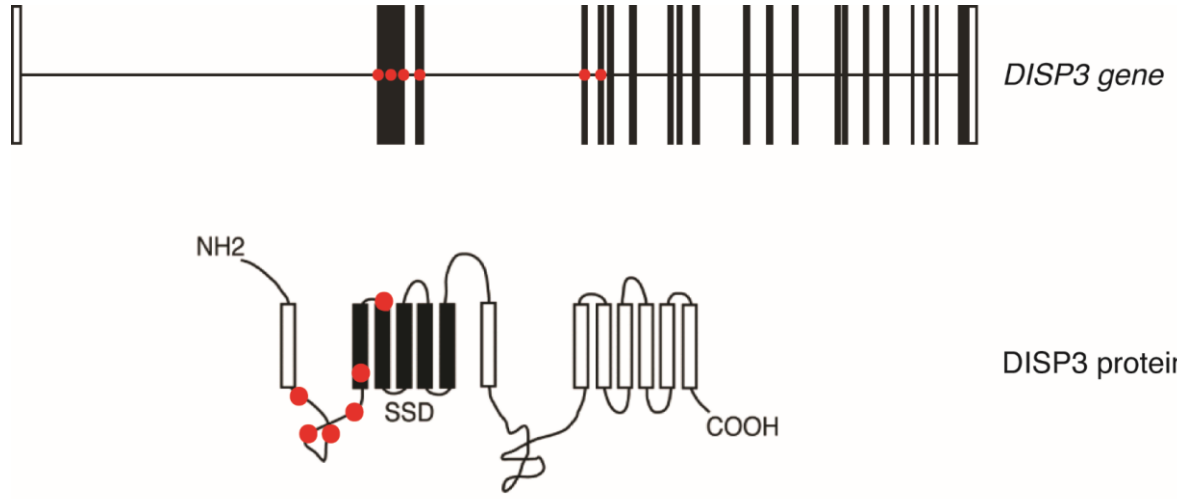

Figure 4.13. The scheme indicates sites of individual CRISPR targets within both *DISP3* gene and protein.

In this knock-out experiment we used CRISPR-Cas9 lentiviral transduction system to perform sequence specific frameshift mutations (Shalem, Sanjana et al. 2014). We prepared pLentiCRISPR constructs encoding each Loop1.1, Loop1.2, Loop1.3, Loop1.4, SSD4 and SSD5 specific CRISPR gRNA.

At the beginning, we transfected HEK 293 FT cells with individual pLentiCRISPR constructs to analyse gRNA efficiency. For analysis of desired regions of genomic DNA, we performed PCR of the CRISPR target genomic regions and then we subcloned and sequenced the reaction product. Under alignment, we observed mutations within target sequences of individual CRISPRs (Figure 4.14). At the Loop 1.1, Loop 1.2 and SSD4 cutting sites we observed huge deletions in all of the sequenced samples, suggesting that CRISPR efficiency in these cases was high. At the Loop 1.4, we observed both deletion and insertion mutations as well as non - mutated sequences, suggesting that CRISPR Loop 1.4 is also efficient (Figure 4.14). At the Loop 1.3 cutting site there were no mutations. Unfortunately, we did not confirm SSD5 cutting site as we were not able to obtain specific PCR product. Therefore, we decided to use pLentiCRISPR - Loop 1.1, Loop 1.2, Loop 1.4 and SSD4 constructs in our experiments.

Next, we transduced D341 cells with chosen pLentiCRISPR viruses and used T7 endonuclease assay to analyse whether transduced cells also bear *DISP3* gene mutations. All our transductions were functional and our CRISPRs specifically introduced mutations which we proved by T7 endonuclease assay (Figure 4.15).

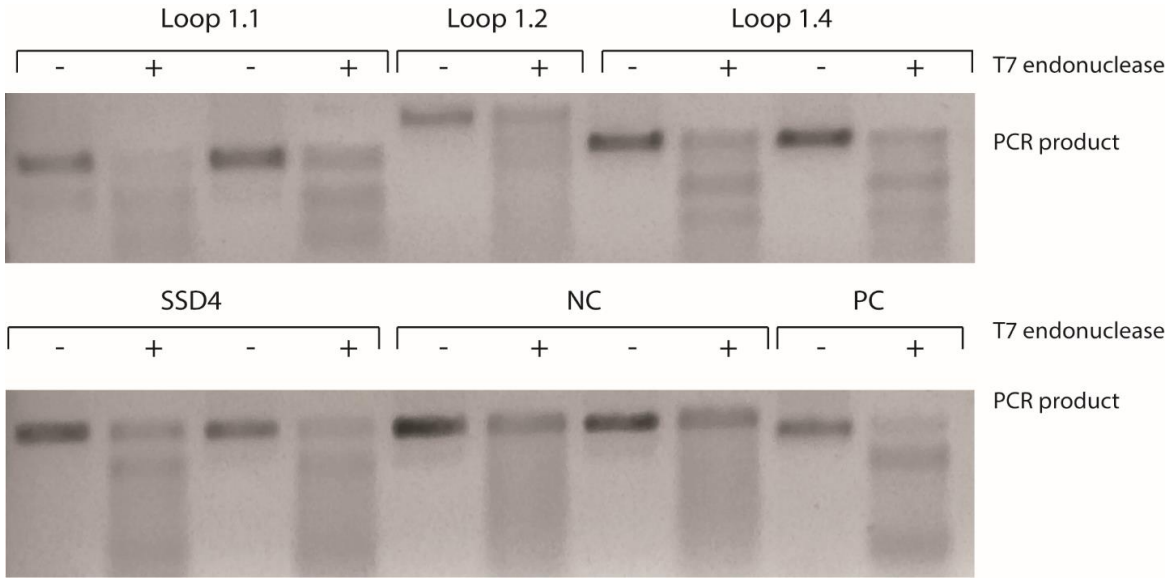

Figure 4.15. The picture shows analysis of mutations within individual CRISPR target sites in pLentiCRISPRs transduced D341 cells. Mutations were analysed by T7 endonuclease assay, NC indicates negative control - D341 cells transduced by empty vector, PC indicates positive control.

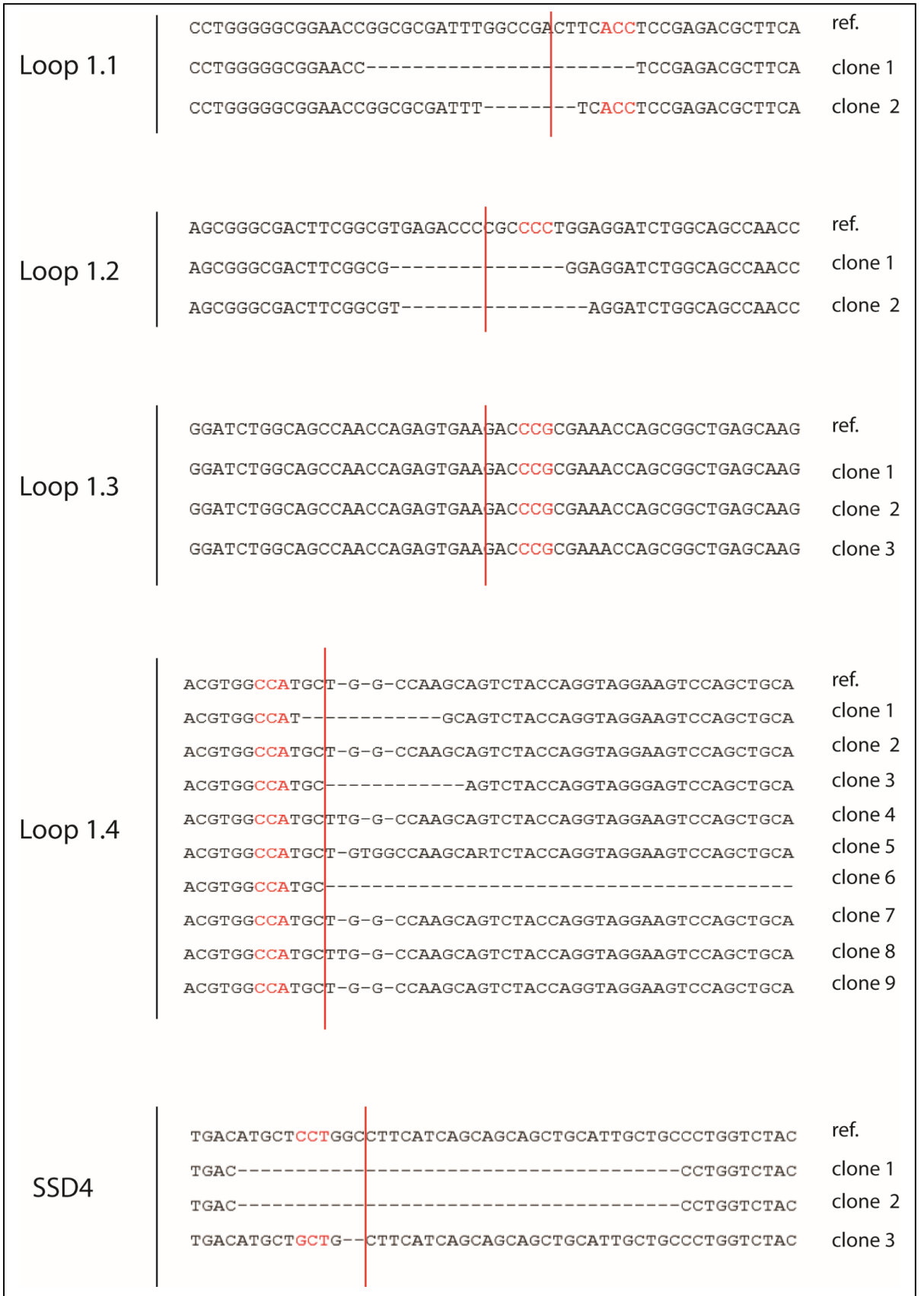

Figure 4.14. The scheme shows sequencing analysis of CRISPR target sites within individual pLentiCRISPRs transduced HEK293FT cells. Red bars indicates exptected CRISPR cutting site. PAM sequence is indicated by red colour.

Next we performed qRT-PCR to analyse *DISP3* expression in *DISP3* mutated D341 cells, empty pLentiCRISPR vector was used as a control. We observed lower expression in all of the *DISP3* mutated cultures. *DISP3* expression was 0,7 - fold lower in Loop 1.1 cell culture, 0,8 – fold lower in Loop 1.2 cell culture, 0,7 – fold lower in Loop 1.4 cell culture and 0,5 – fold lower in SSD4 cell culture (Figure 4.16).

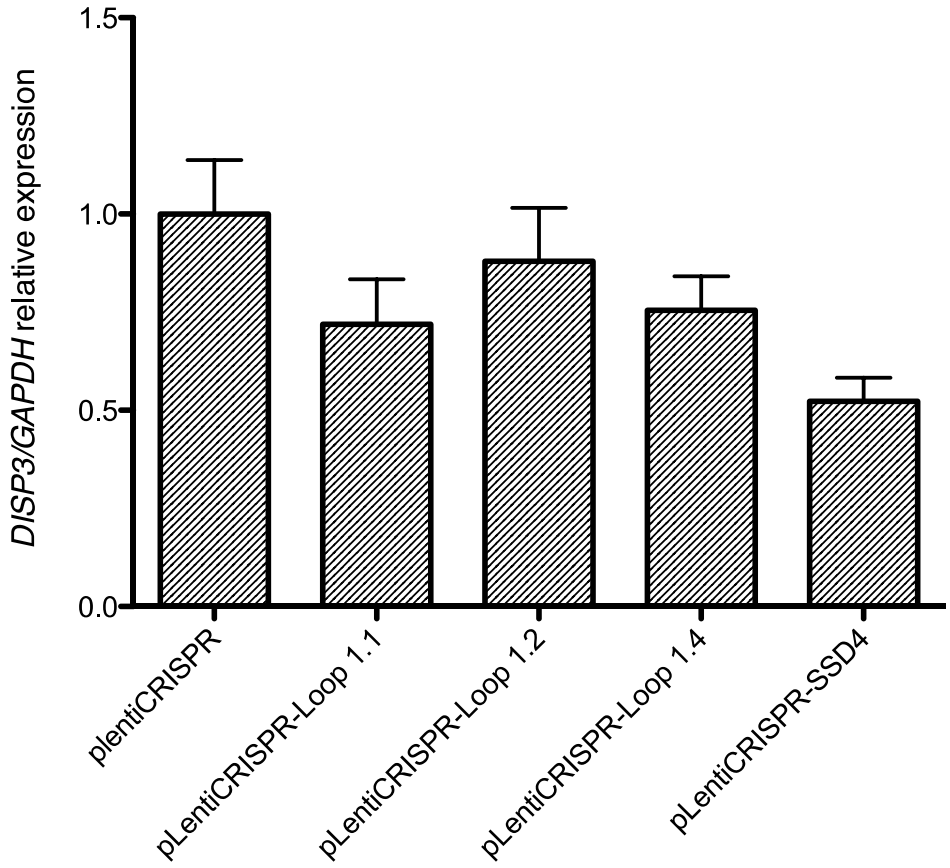

Figure 4.16. The graph shows *DISP3* expression within individual pLentiCRISPRs transduced D341 cells. The data were normalized to D341 cells transduced by empty vector. Error bars represent standard deviation.

When we proved that *DISP3* mutations also diminished *DISP3* expression level. We continued with proliferation measurement. We performed ^{3}H – Thymidine incorporation experiment with all of the variants of *DISP3* mutated cells and we used cells transduced with empty pLentiCRISPR vector as a control. We observed significantly lower incorporation in most of our mutated cell cultures (Figure 4.17).

The cell culture with Loop 1.1 induced mutations revealed 0,8 – fold lower thymidine incorporation compared to a control as well as Loop 1.2 induced mutation cell culture. The cell culture with Loop 1.4 induced mutation showed 0,7 – fold decrease in thymidine incorporation compared to a control. However, cells with the last and most downstream, SSD4 induced mutated site revealed no changes in thymidine incorporation (Figure 4.17).

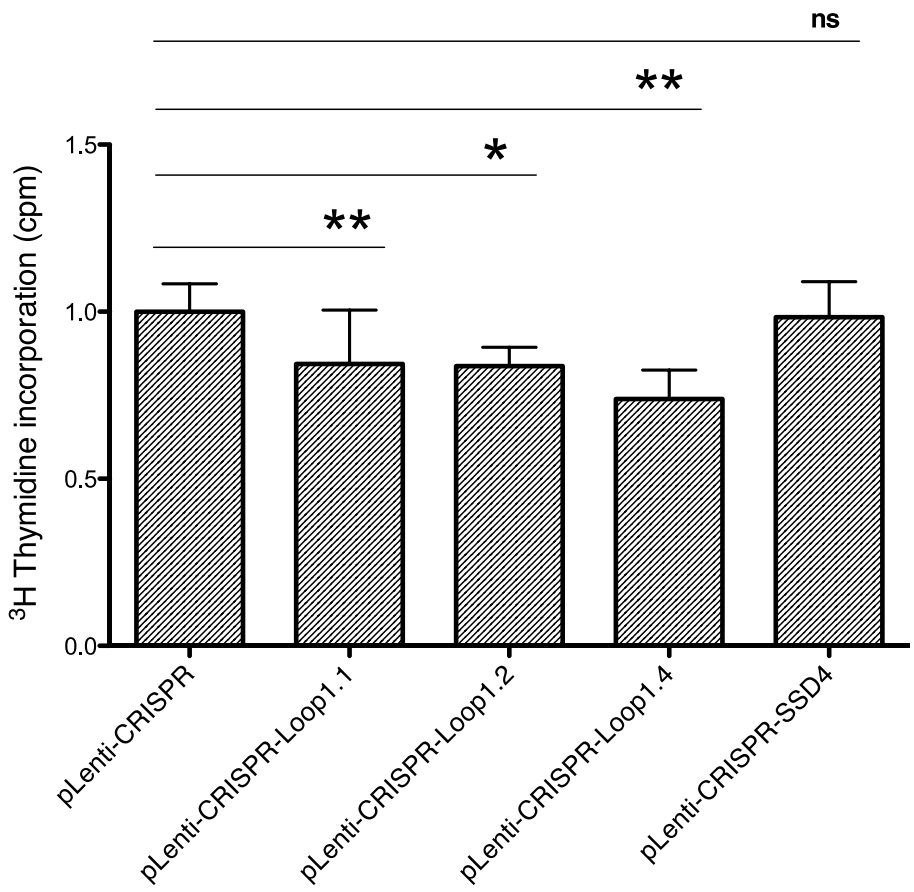

Figure 4.17. The graph shows ^{3}H-Thymidine incorporation in individual pLentiCRISPRs transduced D341 cells. The data were normalized to D341 cell transduced by empty vector. Error bars represent standard deviation.

Finally, when we observed that cells with more upstream *DISP3* mutations have significantly lower proliferation rate, we started to ask whether these cells also differ in their cell cycle profile. Thus, we stained D341 cells with individual *DISP3* mutations with propidium iodide and analysed them by flow cytometry, cells transduced by empty pLentiCRISPR vector were used as a control (Figure 4.18).

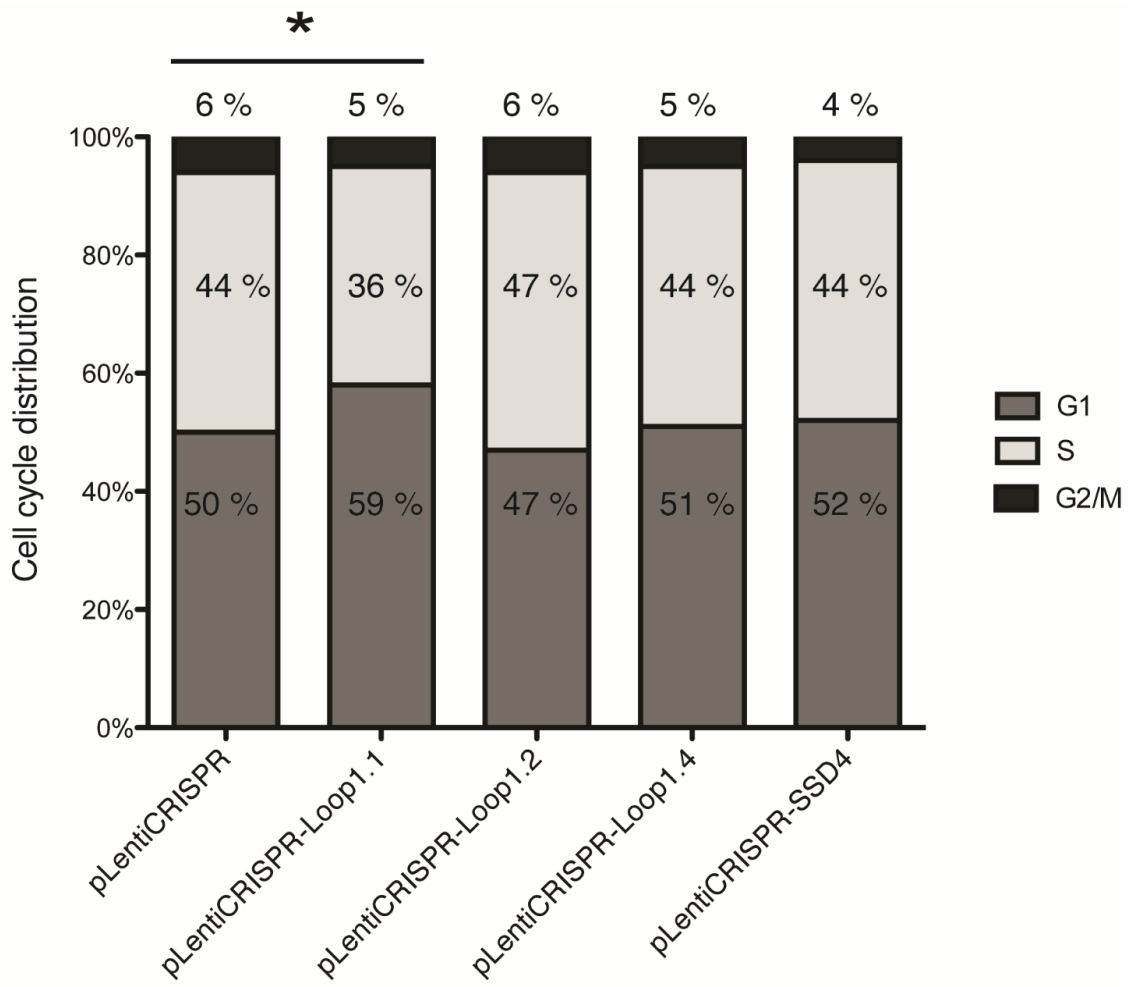

Figure 4.18. The graph shows cell cycle profile of D341 cells transduced by chosen pLentiCRISPR viruses.

We observed a common cell cycle profile in our control cells, where most of the cells were in the G1 phase – specifically it was 50 % of control cells. The second most abundant cell phase was S phase, where we observed 44 % of control cells. The minority of cells stayed within G2 phase, in our case it was 6 % of the cells.

When we compared the cell cycle profile of our *DISP3* – mutated cells, we did not observe any notable changes in their profile in the case of Loop 1.2, Loop 1.4 and SSD4 mutations. However, in the case of most upstream Loop 1.1 mutation we observed a difference in the cell cycle profile compared to control - 59 % cells were in G1 phase and in consistency with that only 36 % of cells were in S phase.

5. Discussion

In this thesis we study role of DISP3 in cell proliferation. First, we confirmed DISP3 predominant expression in human medulloblastoma and retinoblastoma cell lines, which is in consistency with previous findings that DISP3 is mainly expressed in neural and retinal tissues (Zikova, Corlett et al. 2009). In human medulloblastoma we observed increased expression in D341 and D425 cell lines. In contrast, DAOY cell line showed very low level of DISP3 expression. These findings made D341 and DAOY medulloblastoma cell lines suitable for knock-out and overexpression studies.

Medulloblastoma is a highly common and malignant pediatric brain tumour, arising within cerebellum. It is subdivided into 4 subgroups according to its molecular biology background – SHH, WNT, 3 and 4, where the third and fourth subgroups are not very well characterized. Our ArrayExpress analysis of several datasets revealed significant increase in DISP3 expression within all subgroups of medulloblastoma, when compared to normal adult cerebellum and other brain tumours. Comparing each medulloblastoma subgroups, DISP3 was predominantly expressed within subgroup 4. This finding is in consistency with our previous observation, where we used qRT-PCR and immunohistochemistry staining to analyse our set of medulloblastoma patient samples (preliminary data, not published, Figure 2.4).

Although our immunohistochemical analysis contained only limited number of samples, together with the data from ArrayExpress analysis strongly suggests that DISP3 plays role in medulloblastoma tumours properties and, after further evidence, may serve as a marker for medulloblastoma subgroup 4.

Furthermore, we wanted to analyse what role DISP3 expression may play in tumour properties of medulloblastoma. As increased cell proliferation is a major sign of cancer cells, we first started to ask whether DISP3 expression affects cell proliferation. In our study we used DAOY cells to overexpress DISP3 and measured ^{3}H-Thymidine incorporation. We observed 2-fold increase of ^{3}H-Thymidine incorporation in DISP3 expressing cells compared to theby asymmetrical division control. These data suggest that DISP3 may affect cell properties inducing its proliferation.

To prove our findings, we used C 17.2 mouse neural progenitor cell line with low expression of *DISP3* to perform another overexpression experiment. The C 17.2 cell line was derived from EGL zone of mouse cerebellum and keeps part of its properties also *in vitro*, as it is capable of differentiation into neurons and astrocytes (Snyder, Deitcher et al. 1992, Lundqvist, El Andaloussi-Lilja et al. 2013). EGL zone of cerebellum is part of the brain where neural progenitors undergo massive proliferation and afterwards they differentiate into neurons and glia. It was shown that dysregulation of this process may lead to cancer progression and medulloblastoma formation (Schuller, Heine et al. 2008). This background makes C 17.2 cells a very good model for studies of medulloblastoma formation. Here we show that overexpression of DISP3 within C 17.2 cells promotes their proliferation as we observed 1,7-fold increase of ^{3}H- Thymidine incorporation within C 17.2 cells expressing DISP3 in comparison to the control. These data thus proved our observation within DAOY cells and suggests, that overexpression of DISP3 plays role in medulloblastoma cancer progression.

As it was shown that some medulloblastoma arise from neural progenitors (Schuller, Heine et al. 2008, Yang, Ellis et al. 2008) and also medulloblastoma itself reveals stem-like properties (Hemmati, Nakano et al. 2003), we wanted to analyse whether DISP3 overexpression affects this ability. We overexpressed DISP3 in C 17.2 cells and analysed their ability to differentiate into neurons and astrocytes. Upon differentiation conditions, we observed morphological changes of control cells earlier then in DISP3 expressing cells and morphology of both cells was still different at the end of the differentiation period. These observations suggest that DISP3 expression leads to delay in differentiation and this process could be accompanied by its higher proliferation as we measured before.

We proved that C 17.2 cells differentiated into neurons and astrocytes, as we measured increase in βIII-tubulin and GFAP expression and expected decrease in Nestin expression. Delay in differentiation of DISP3 expressing C 17.2 cells was apparent in all of the three markers. At the beginning of differentiation, Nestin expression was higher in DISP3 expressing cells compared to the control and this difference then gradually decreased, in the end of differentiation period Nestin expression became the same in both cells. These data show that DISP3 expression has negative effect on cell willingness to leave progenitor fate.

Similar result was shown when we analysed GFAP expression. C 17.2 cells with DISP3 expression revealed less GFAP expression during whole differentiation when compared to control cells. When we analysed βIII-tubulin expression, we observed that DISP3 expressing cells followed the expression pattern of control cells, however, βIII-tubulin expression was significantly lower in all stages of the differentiation period.

Together, these data show that C 17.2 cells with DISP3 ectopic expression undergo neuronal and glial differentiation more slowly than control cells but DISP3 expression itself is not sufficient to block the differentiation completely. In context of neurodevelopmental origin of distinct medulloblastoma, all these data suggest that DISP3 dysregulated expression may play role in medulloblastoma formation, as it promotes cell proliferation and delays its differentiation.

Consequently, we asked whether also lack of DISP3 expression will lead to diminished proliferation and thus negatively affect cancerous properties of medulloblastoma cells. In our experiments we induced several mutations within *DISP3* gene by CRISPR-Cas9 system in D341 medullublastoma cell line with increased expression of DISP3. Concomitantly, we analysed ^{3}H-Thymidine incorporation similarly as in previous overexpression experiments and observed decrease in cell proliferation. When we induced *DISP3* mutations within Loop1.1, Loop1.2 and Loop1.4 sites, proliferation rate was 0,7 – 0,8-fold lower than in control cells. In contrast, when we induced mutation within SSD4 site proliferation was not changed.

Cell proliferation depends on the ability of the cell to get through the cell cycle and its checkpoints. Therefore, we asked whether *DISP3* mutations have effect on this ability. We measured cell cycle profile of each *DISP3* mutant cells and control cells. In the case of Loop1.1 mutation we observed that cells rather persisted within G1 phase. This may suggest that *DISP3* Loop 1.1 mutation affect ability of D341 cells to pass the G1/S phase checkpoint. However, this ability was not affected by any other mutation sites, even if it was located within the first luminal loop.

Possible reason for differences between each mutated cell cultures may be the mechanism of knock-out performed by CRISPR-Cas9 system. As Cas9 endonuclease induces doublestrand DNA breaks, we assumed that DNA repair mechanism represented by

non-homologous end joining (NHEJ) pathway will induce insertion or deletion mutations (Davis and Chen 2013). Although we confirmed the ability of our specific gRNAs to induce mutations in our experiments and used only capable guides, gene manipulation itself may not be sufficient for abortion of DISP3 expression.

We assumed that frameshift caused by NHEJ pathway make premature stop codons and these will be then recognised and degraded by non-sense mediated decay pathway. However, efficiency of this process is not the same for all the transcripts and some of the premature stop codons may not be recognised at all (Lappalainen, Sammeth et al. 2013).

To prove whether *DISP3* transcript is getting degraded in our cells, we performed qRT-PCR and observed decrease in *DISP3* expression within all of the versions of *DISP3* mutations. Thus we concluded that all of our mutated transcripts are recognised by non-sense mediated decay and degraded and it probably does not cause observed difference in D341 cell proliferation.

Another possible reason might be that the rest of the present mutated *DISP3* transcripts are still translated and produce aberrant, somehow more stable, protein forms. In this case, Loop1.1, Loop1.2 and Loop1.4 mutated D341 cells would produce short DISP3 protein with one transmembrane domain and different lengths of the first loop. However, in the case of SSD4 mutated D341 cells aberrant DISP3 protein would consist of the first transmembrane segment, intact luminal loop and part of SSD transmembrane domain. This may suggest, that protein domain responsible for the phenotype is localized within the first luminal loop, as proliferation is not affected only in the cells with intact luminal loop. However, to make this conclusion, we would need further evidence on protein expression.

Next, as CRISPR-Cas9 system in our settings induce mutations randomly, cell culture after antibiotic selection still contains numerous mix of different *DISP3* transcripts. To avoid that clonal selection of mutated cells would be necessary. However, our efforts to produce *DISP3* clonal mutants failed so far and we thus preformed our experiments within the cell mixture and that could also be the reason for slightly different results in the different mutated cell lines we used.

Moreover, in the case of CRISPR-Cas9 system mediated genome editing, there are controversies about off-target effects of gRNAs. These can also recognize sequences with several mismatches (Lin, Cradick et al. 2014). This feature of CRISPR-Cas9 system can thus affect the phenotype and cause differences in our observations. Because off-target prediction tools were not available at the beginning of our experiment, we analysed our gRNAs retrospectively. We used Off-Spotter and analysed possible off-targets with up to 3 mismatches (Pliatsika and Rigoutsos 2015). The amount of possible off-targets is luckily rather small, all of our gRNAs do not reveal any target sequences for 1 and 2 mismatches and in the case of 3 mismatches they reveal up to 13 off-targets with no overlaps. These findings suggest that our observations were not caused by off-target effect of CRISPR-Cas9 system.

Taken together, our data show that DISP3 affect cell proliferation of medulloblastoma cells in two ways. DISP3 overexpression leads to promotion of cell proliferation and DISP3 diminished expression leads to decrease in cell proliferation. This suggests that DISP3 increased expression in subgroup 4 medulloblastoma patients can have effect on tumour properties and progression.

Moreover, microarray gene expression analysis of C 17.2 cells with DISP3 overexpression revealed *EPB4.1L3* and *PRELP* genes, expression of which was significantly reduced (Zikova, Konirova et al. 2014). EPB4.1L3 is a member of a protein family involved in linking of transmembrane glycoproteins to actin cytoskeleton and thus affecting many cellular processes such as cell proliferation, polarization or migration. All these processes are involved in tumour progression and it was shown that in highly metastatic prostate cancer, Epb4.1l3 is reduced (Wong, Haack et al. 2007). Similarly, PRELP was found as counteracting factor in formation of bone and visceral metastasis formation in breast cancer (Rucci, Capulli et al. 2013). These data thus suggest that DISP3 expression in medulloblastoma affects also its metastatic potential by suppression of tumour supressors.

6. Conclusion

In this thesis, we focused on DISP3 role in cell proliferation *in vitro*. We generated DISP3 stable ectopic expression within DAOY medulloblastoma cells and C 17.2 neural progenitor cells. We analysed DISP3 effect on cell proliferation and observed 2-fold increase in proliferation of DAOY, and 1,7-fold increase in proliferation of C 17.2 cells.

Next, we analysed level of DISP3 expression in differentiation of C 17.2 cells into neurons and astrocytes. We applied successful differentiation conditions and observed both neuronal and astrocytic differentiation in control cells. C 17.2 cells with DISP3 ectopic expression showed delay in this process. This we confirmed by Nestin, βIII-tubulin and GFAP analysis using qRT-PCR and immunofluorescence staining.

Further, we analysed *DISP3* gene and chose 6 possible CRISPR target sequences within several exons. We cloned pLentiCRISPR constructs encoding Cas9 endonuclease and individual gRNA that targets chosen sequences. Cutting efficiency of individual constructs, we then confirmed by sequencing of target sites. Next, we used four efficient pLentiCRISPR constructs to generate *DISP3* mutations in the D341 medulloblastoma cell line within 4 different sites. Successful mutagenesis we proved by T7 endonuclease assay.

Finally, we analysed cell proliferation of individual *DISP3* mutants and observed 0,7- to 0,8 -fold diminished cell proliferation within three of four mutated cell cultures. Moreover, we analysed cell cycle profile of individual *DISP3* mutants. Only one of four mutated sites demonstrated changes in the profile showing that cells rather persisted in G1 phase.

Taken together, our data show that DISP3 ectopic expression promotes cell proliferation and leads to a delay in neural differentiation. Similarly, DISP3 reduced expression leads to decrease in cell proliferation.

7. References

Altmann, S. W., H. R. Davis, Jr., L. J. Zhu, X. Yao, L. M. Hoos, G. Tetzloff, S. P. Iyer, M. Maguire, A. Golovko, M. Zeng, L. Wang, N. Murgolo and M. P. Graziano (2004). "Niemann-Pick C1 Like 1 protein is critical for intestinal cholesterol absorption." Science **303**(5661): 1201-1204.

Bae, S. H., J. N. Lee, B. U. Fitzky, J. Seong and Y. K. Paik (1999). "Cholesterol biosynthesis from lanosterol. Molecular cloning, tissue distribution, expression, chromosomal localization, and regulation of rat 7-dehydrocholesterol reductase, a Smith-Lemli-Opitz syndrome-related protein." J Biol Chem **274**(21): 14624-14631.

Bignami, A. and D. Dahl (1974). "Astrocyte-specific protein and neuroglial differentiation. An immunofluorescence study with antibodies to the glial fibrillary acidic protein." J Comp Neurol **153**(1): 27-38.

Brown, M. S., J. R. Faust and J. L. Goldstein (1975). "Role of the low density lipoprotein receptor in regulating the content of free and esterified cholesterol in human fibroblasts." J Clin Invest **55**(4): 783-793.

Brown, M. S. and J. L. Goldstein (2009). "Cholesterol feedback: from Schoenheimer's bottle to Scap's MELADL." J Lipid Res **50 Suppl**: S15-27.

Butts, T., N. Chaplin and R. J. Wingate (2011). "Can clues from evolution unlock the molecular development of the cerebellum?" Mol Neurobiol **43**(1): 67-76.

Cheng, S. Y., J. L. Leonard and P. J. Davis (2010). "Molecular aspects of thyroid hormone actions." Endocr Rev **31**(2): 139-170.

Cho, M. K. (2015). "Thyroid dysfunction and subfertility." Clin Exp Reprod Med **42**(4): 131-135.
Dahlstrand, J., M. Lardelli and U. Lendahl (1995). "Nestin mRNA expression correlates with the central nervous system progenitor cell state in many, but not all, regions of developing central nervous system." Brain Res Dev Brain Res **84**(1): 109-129.

Davis, A. J. and D. J. Chen (2013). "DNA double strand break repair via non-homologous end-joining." Transl Cancer Res **2**(3): 130-143.

Duncan, E. A., M. S. Brown, J. L. Goldstein and J. Sakai (1997). "Cleavage site for sterol-regulated protease localized to a leu-Ser bond in the lumenal loop of sterol regulatory element-binding protein-2." J Biol Chem **272**(19): 12778-12785.

Eng, L. F., J. J. Vanderhaeghen, A. Bignami and B. Gerstl (1971). "An acidic protein isolated from fibrous astrocytes." Brain Res **28**(2): 351-354.

Frederiksen, K. and R. D. McKay (1988). "Proliferation and differentiation of rat neuroepithelial precursor cells in vivo." J Neurosci **8**(4): 1144-1151.

Friedman, H. S., P. C. Burger, S. H. Bigner, J. Q. Trojanowski, G. M. Brodeur, X. M. He, C. J. Wikstrand, J. Kurtzberg, M. E. Berens, E. C. Halperin and et al. (1988). "Phenotypic and genotypic analysis of a human medulloblastoma cell line and transplantable xenograft (D341 Med) demonstrating amplification of c-myc." Am J Pathol **130**(3): 472-484.

Gibson, P., Y. Tong, G. Robinson, M. C. Thompson, D. S. Currle, C. Eden, T. A. Kranenburg, T. Hogg, H. Poppleton, J. Martin, D. Finkelstein, S. Pounds, A. Weiss, Z. Patay, M. Scoggins, R. Ogg, Y. Pei, Z. J. Yang, S. Brun, Y. Lee, F. Zindy, J. C. Lindsey, M. M. Taketo, F. A. Boop, R. A. Sanford, A. Gajjar, S. C. Clifford, M. F. Roussel, P. J. McKinnon, D. H. Gutmann, D. W. Ellison, R. Wechsler-Reya and R. J. Gilbertson (2010). "Subtypes of medulloblastoma have distinct developmental origins." Nature **468**(7327): 1095-1099.

Goldstein, J. L. and M. S. Brown (1990). "Regulation of the mevalonate pathway." Nature **343**(6257): 425-430.

Gutleb, A. C., S. Cambier and T. Serchi (2016). "Impact of Endocrine Disruptors on the Thyroid Hormone System." Horm Res Paediatr.

Hammes, S. R. and P. J. Davis (2015). "Overlapping nongenomic and genomic actions of thyroid hormone and steroids." Best Pract Res Clin Endocrinol Metab **29**(4): 581-593.

Hemmati, H. D., I. Nakano, J. A. Lazareff, M. Masterman-Smith, D. H. Geschwind, M. Bronner-Fraser and H. I. Kornblum (2003). "Cancerous stem cells can arise from pediatric brain tumors." Proc Natl Acad Sci U S A **100**(25): 15178-15183.

Hua, X., C. Yokoyama, J. Wu, M. R. Briggs, M. S. Brown, J. L. Goldstein and X. Wang (1993). "SREBP-2, a second basic-helix-loop-helix-leucine zipper protein that stimulates transcription by binding to a sterol regulatory element." Proc Natl Acad Sci U S A **90**(24): 11603-11607.

Jacobsen, P. F., D. J. Jenkyn and J. M. Papadimitriou (1985). "Establishment of a human medulloblastoma cell line and its heterotransplantation into nude mice." J Neuropathol Exp Neurol **44**(5): 472-485.

Katoh, Y. and M. Katoh (2005). "Identification and characterization of DISP3 gene in silico." Int J Oncol **26**(2): 551-556.

Khatua, S. (2016). "Evolving molecular era of childhood medulloblastoma: time to revisit therapy." Future Oncol **12**(1): 107-117.

Kuwabara, P. E. and M. Labouesse (2002). "The sterol-sensing domain: multiple families, a unique role?" Trends Genet **18**(4): 193-201.

Kwon, H. J., L. Abi-Mosleh, M. L. Wang, J. Deisenhofer, J. L. Goldstein, M. S. Brown and R. E. Infante (2009). "Structure of N-terminal domain of NPC1 reveals distinct subdomains for binding and transfer of cholesterol." Cell **137**(7): 1213-1224.

Laguesse, S., E. Peyre and L. Nguyen (2015). "Progenitor genealogy in the developing cerebral cortex." Cell Tissue Res **359**(1): 17-32.

Lappalainen, T., M. Sammeth, M. R. Friedlander, P. A. t Hoen, J. Monlong, M. A. Rivas, M. Gonzalez-Porta, N. Kurbatova, T. Griebel, P. G. Ferreira, M. Barann, T. Wieland, L. Greger, M. van Iterson, J. Almlof, P. Ribeca, I. Pulyakhina, D. Esser, T. Giger, A. Tikhonov, M. Sultan, G. Bertier, D. G. MacArthur, M. Lek, E. Lizano, H. P. Buermans, I. Padioleau, T. Schwarzmayr, O. Karlberg, H. Ongen, H. Kilpinen, S. Beltran, M. Gut, K. Kahlem, V. Amstislavskiy, O. Stegle, M. Pirinen, S. B. Montgomery, P. Donnelly, M. I. McCarthy, P. Flicek, T. M. Strom, C. Geuvadis, H. Lehrach, S. Schreiber, R. Sudbrak, A. Carracedo, S. E. Antonarakis, R. Hasler, A. C. Syvanen, G. J. van Ommen, A. Brazma, T. Meitinger, P.

Rosenstiel, R. Guigo, I. G. Gut, X. Estivill and E. T. Dermitzakis (2013). "Transcriptome and genome sequencing uncovers functional variation in humans." Nature **501**(7468): 506-511.

Lin, Y., T. J. Cradick, M. T. Brown, H. Deshmukh, P. Ranjan, N. Sarode, B. M. Wile, P. M. Vertino, F. J. Stewart and G. Bao (2014). "CRISPR/Cas9 systems have off-target activity with insertions or deletions between target DNA and guide RNA sequences." Nucleic Acids Res **42**(11): 7473-7485.

Liscum, L., R. D. Cummings, R. G. Anderson, G. N. DeMartino, J. L. Goldstein and M. S. Brown (1983). "3-Hydroxy-3-methylglutaryl-CoA reductase: a transmembrane glycoprotein of the endoplasmic reticulum with N-linked "high-mannose" oligosaccharides." Proc Natl Acad Sci U S A **80**(23): 7165-7169.

Liscum, L., J. Finer-Moore, R. M. Stroud, K. L. Luskey, M. S. Brown and J. L. Goldstein (1985). "Domain structure of 3-hydroxy-3-methylglutaryl coenzyme A reductase, a glycoprotein of the endoplasmic reticulum." J Biol Chem **260**(1): 522-530.

Liscum, L., K. L. Luskey, D. J. Chin, Y. K. Ho, J. L. Goldstein and M. S. Brown (1983). "Regulation of 3-hydroxy-3-methylglutaryl coenzyme A reductase and its mRNA in rat liver as studied with a monoclonal antibody and a cDNA probe." J Biol Chem **258**(13): 8450-8455.

Lopez-Espindola, D., C. Morales-Bastos, C. Grijota-Martinez, X. H. Liao, D. Lev, E. Sugo, C. F. Verge, S. Refetoff, J. Bernal and A. Guadano-Ferraz (2014). "Mutations of the thyroid hormone transporter MCT8 cause prenatal brain damage and persistent hypomyelination." J Clin Endocrinol Metab **99**(12): E2799-2804.

Lopez, M. E., A. D. Klein, U. J. Dimbil and M. P. Scott (2011). "Anatomically defined neuron-based rescue of neurodegenerative Niemann-Pick type C disorder." J Neurosci **31**(12): 4367-4378.

Lucas, T. F., A. R. Nascimento, R. Pisolato, M. T. Pimenta, M. F. Lazari and C. S. Porto (2014). "Receptors and signaling pathways involved in proliferation and differentiation of Sertoli cells." Spermatogenesis **4**: e28138.

Lundqvist, J., J. El Andaloussi-Lilja, C. Svensson, H. Gustafsson Dorfh and A. Forsby (2013). "Optimisation of culture conditions for differentiation of C17.2 neural stem cells to be used for in vitro toxicity tests." Toxicol In Vitro **27**(5): 1565-1569.

Marzban, H., N. Hoy, M. Buchok, K. C. Catania and R. Hawkes (2015). "Compartmentation of the cerebellar cortex: adaptation to lifestyle in the star-nosed mole Condylura cristata." Cerebellum **14**(2): 106-118.

Mastracci, T. L. and C. Evans-Molina (2014). "Pancreatic and Islet Development and Function: The Role of Thyroid Hormone." J Endocrinol Diabetes Obes **2**(3).

Moebius, F. F., B. U. Fitzky, J. N. Lee, Y. K. Paik and H. Glossmann (1998). "Molecular cloning and expression of the human delta7-sterol reductase." Proc Natl Acad Sci U S A **95**(4): 1899-1902.

Mohan, V., R. A. Sinha, A. Pathak, L. Rastogi, P. Kumar, A. Pal and M. M. Godbole (2012). "Maternal thyroid hormone deficiency affects the fetal neocorticogenesis by reducing the proliferating pool, rate of neurogenesis and indirect neurogenesis." Exp Neurol **237**(2): 477-488.

Nohturfft, A., M. S. Brown and J. L. Goldstein (1998). "Topology of SREBP cleavage-activating protein, a polytopic membrane protein with a sterol-sensing domain." J Biol Chem **273**(27): 17243-17250.

Nohturfft, A., R. A. DeBose-Boyd, S. Scheek, J. L. Goldstein and M. S. Brown (1999). "Sterols regulate cycling of SREBP cleavage-activating protein (SCAP) between endoplasmic reticulum and Golgi." Proc Natl Acad Sci U S A **96**(20): 11235-11240.

Patrono, C., C. Rizzo, A. Tessa, A. Giannotti, P. Borrelli, R. Carrozzo, F. Piemonte, E. Bertini, C. Dionisi-Vici and F. M. Santorelli (2000). "Novel 7-DHCR mutation in a child with Smith-Lemli-Opitz syndrome." Am J Med Genet **91**(2): 138-140.

Pliatsika, V. and I. Rigoutsos (2015). ""Off-Spotter": very fast and exhaustive enumeration of genomic lookalikes for designing CRISPR/Cas guide RNAs." Biol Direct **10**: 4.

Preau, L., J. B. Fini, G. Morvan-Dubois and B. Demeneix (2015). "Thyroid hormone signaling during early neurogenesis and its significance as a vulnerable window for endocrine disruption." Biochim Biophys Acta **1849**(2): 112-121.

Roskams, A. J., X. Cai and G. V. Ronnett (1998). "Expression of neuron-specific beta-III tubulin during olfactory neurogenesis in the embryonic and adult rat." Neuroscience **83**(1): 191-200.

Rucci, N., M. Capulli, L. Ventura, A. Angelucci, B. Peruzzi, V. Tillgren, M. Muraca, D. Heinegard and A. Teti (2013). "Proline/arginine-rich end leucine-rich repeat protein N-terminus is a novel osteoclast antagonist that counteracts bone loss." J Bone Miner Res **28**(9): 1912-1924.

Sakai, J., E. A. Duncan, R. B. Rawson, X. Hua, M. S. Brown and J. L. Goldstein (1996). "Sterol-regulated release of SREBP-2 from cell membranes requires two sequential cleavages, one within a transmembrane segment." Cell **85**(7): 1037-1046.

Sakai, J., A. Nohturfft, D. Cheng, Y. K. Ho, M. S. Brown and J. L. Goldstein (1997). "Identification of complexes between the COOH-terminal domains of sterol regulatory element-binding proteins (SREBPs) and SREBP cleavage-activating protein." J Biol Chem **272**(32): 20213-20221.

Samkari, A., J. C. White and R. J. Packer (2015). "Medulloblastoma: toward biologically based management." Semin Pediatr Neurol **22**(1): 6-13.

Schuller, U., V. M. Heine, J. Mao, A. T. Kho, A. K. Dillon, Y. G. Han, E. Huillard, T. Sun, A. H. Ligon, Y. Qian, Q. Ma, A. Alvarez-Buylla, A. P. McMahon, D. H. Rowitch and K. L. Ligon (2008). "Acquisition of granule neuron precursor identity is a critical determinant of progenitor cell competence to form Shh-induced medulloblastoma." Cancer Cell **14**(2): 123-134.

Shalem, O., N. E. Sanjana, E. Hartenian, X. Shi, D. A. Scott, T. S. Mikkelsen, D. Heckl, B. L. Ebert, D. E. Root, J. G. Doench and F. Zhang (2014). "Genome-scale CRISPR-Cas9 knockout screening in human cells." Science **343**(6166): 84-87.

Singh, S. K., I. D. Clarke, M. Terasaki, V. E. Bonn, C. Hawkins, J. Squire and P. B. Dirks (2003). "Identification of a cancer stem cell in human brain tumors." Cancer Res **63**(18): 5821-5828.

Snyder, E. Y., D. L. Deitcher, C. Walsh, S. Arnold-Aldea, E. A. Hartwieg and C. L. Cepko (1992). "Multipotent neural cell lines can engraft and participate in development of mouse cerebellum." Cell **68**(1): 33-51.

Vanier, M. T. (2015). "Complex lipid trafficking in Niemann-Pick disease type C." J Inherit Metab Dis **38**(1): 187-199.

Wang, X., R. Sato, M. S. Brown, X. Hua and J. L. Goldstein (1994). "SREBP-1, a membrane-bound transcription factor released by sterol-regulated proteolysis." Cell **77**(1): 53-62.

Wong, S. Y., H. Haack, J. L. Kissil, M. Barry, R. T. Bronson, S. S. Shen, C. A. Whittaker, D. Crowley and R. O. Hynes (2007). "Protein 4.1B suppresses prostate cancer progression and metastasis." Proc Natl Acad Sci U S A **104**(31): 12784-12789.

Wustner, D. and K. Solanko (2015). "How cholesterol interacts with proteins and lipids during its intracellular transport." Biochim Biophys Acta **1848**(9): 1908-1926.

Yang, Z. J., T. Ellis, S. L. Markant, T. A. Read, J. D. Kessler, M. Bourboulas, U. Schuller, R. Machold, G. Fishell, D. H. Rowitch, B. J. Wainwright and R. J. Wechsler-Reya (2008). "Medulloblastoma can be initiated by deletion of Patched in lineage-restricted progenitors or stem cells." Cancer Cell **14**(2): 135-145.

Yokoyama, C., X. Wang, M. R. Briggs, A. Admon, J. Wu, X. Hua, J. L. Goldstein and M. S. Brown (1993). "SREBP-1, a basic-helix-loop-helix-leucine zipper protein that controls transcription of the low density lipoprotein receptor gene." Cell **75**(1): 187-197.

Zikova, M., A. Corlett, Z. Bendova, P. Pajer and P. Bartunek (2009). "DISP3, a sterol-sensing domain-containing protein that links thyroid hormone action and cholesterol metabolism." Mol Endocrinol **23**(4): 520-528.

Zikova, M., J. Konirova, K. Ditrychova, A. Corlett, M. Kolar and P. Bartunek (2014). "DISP3 promotes proliferation and delays differentiation of neural progenitor cells." FEBS Lett **588**(21): 4071-4077.